Supporting Information

For

Non-covalent Interactions in Molecular Architecture and Solvent Free Catalytic Activity Towards CO_2 Fixation of Mononuclear Co(III) Complexes Installed on Modified Schiff Base Ligands

Souvik Barman[a], Dhiraj Das[a,b] and Kuntal Pal[*a]

Department of Chemistry, University of Calcutta, 92 APC Road, Kolkata 700009, India

Contents

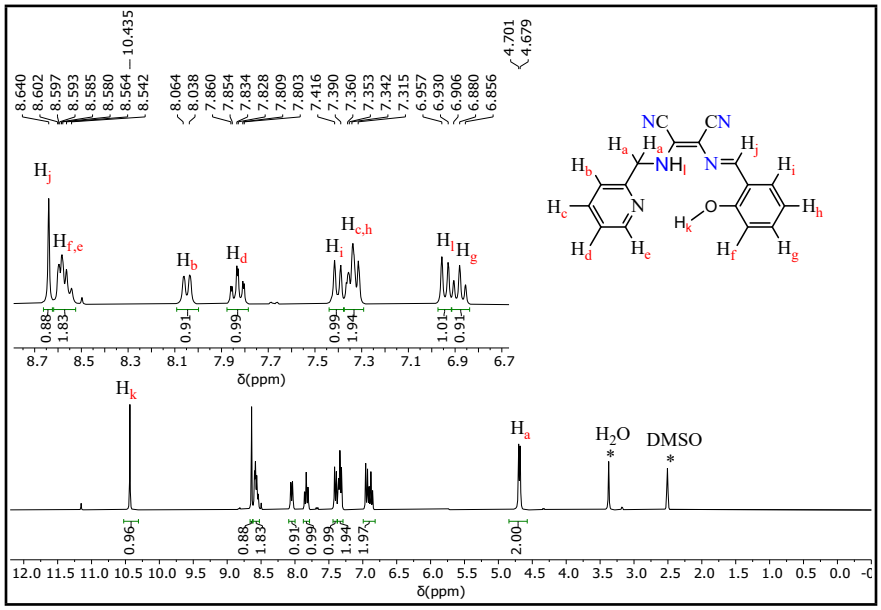

Fig. S1:[1]H NMR Spectrum of $\mathbf{H_2L^H}$ in DMSO- d_6.

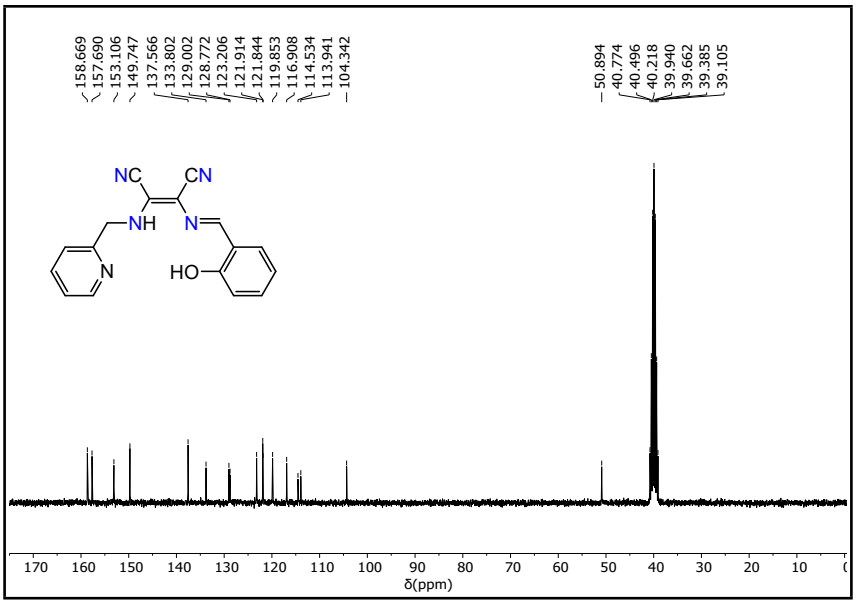

Fig. S2: ^{13}C NMR Spectrum of $\mathbf{H_2L^H}$ in DMSO- d_6.

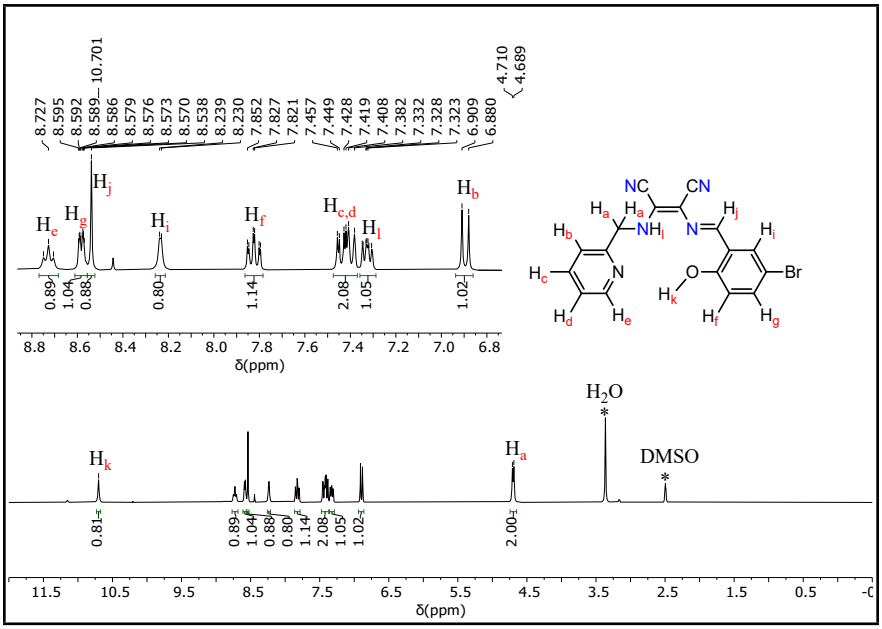

Fig. S3: ^{1}H NMR Spectrum of $\mathbf{H_2L^{Br}}$ in DMSO- d_6.

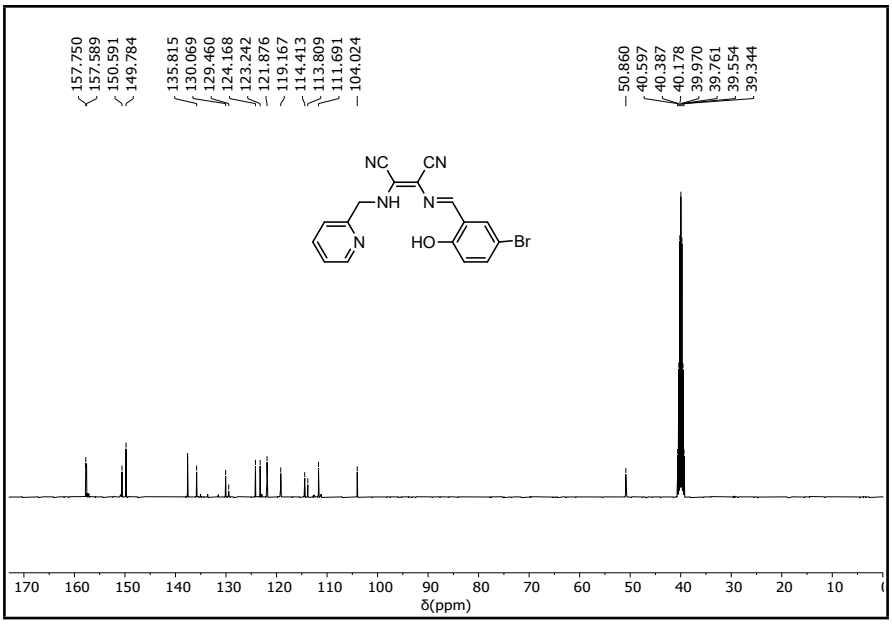

Fig. S4: ^{13}C NMR Spectrum of $\mathbf{H_2L^{Br}}$ in DMSO- d_6.

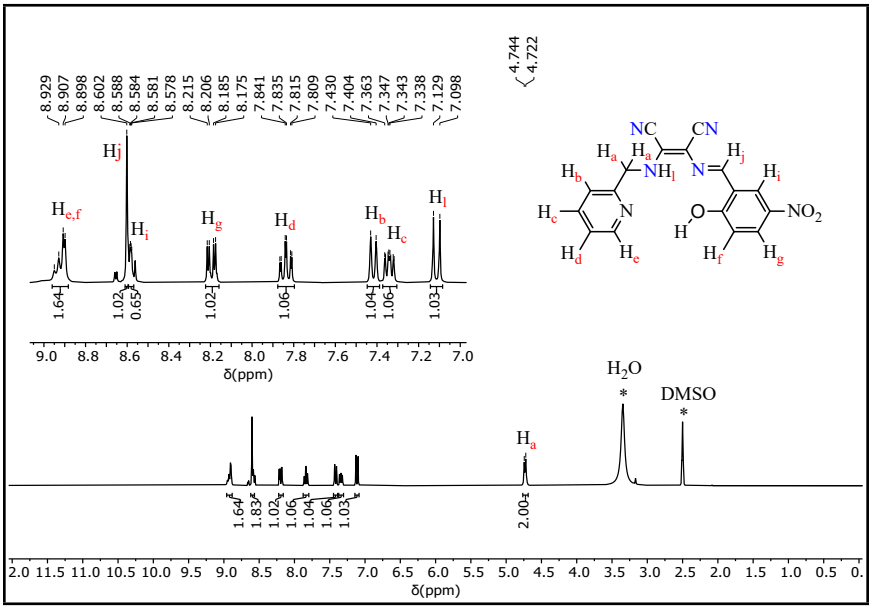

Fig. S5: ^{1}H NMR Spectrum of $\mathbf{H_2L^{NO2}}$ in DMSO- d_6.

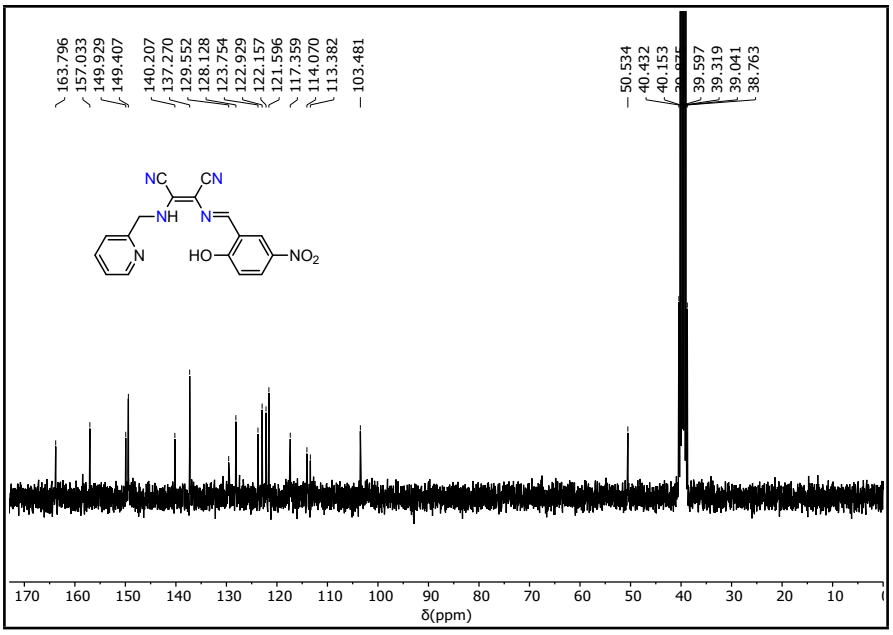

Fig. S6: ^{13}C NMR Spectrum of $\mathbf{H_2L^{NO2}}$ in DMSO- d_6.

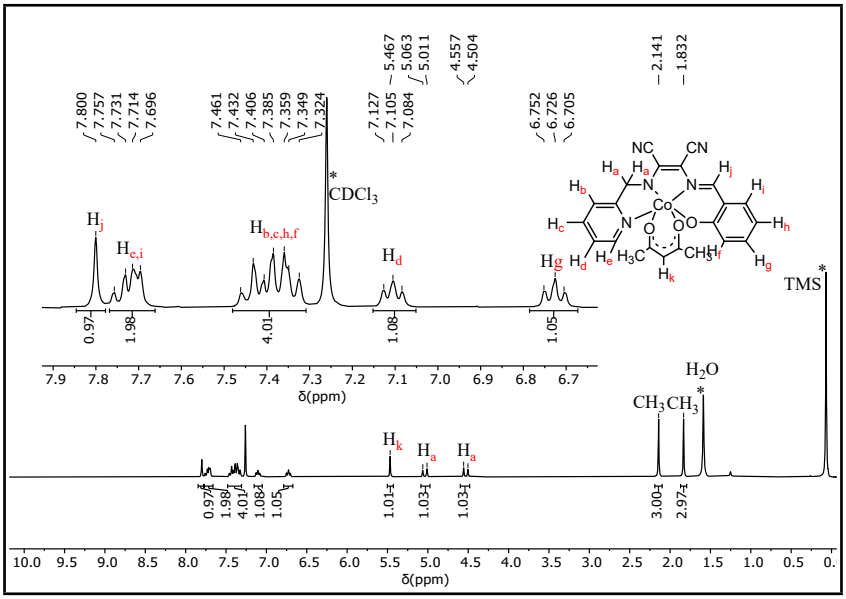

Fig. S7: ^{1}H NMR Spectrum of **Co-1^{H}** in $CDCl_3$.

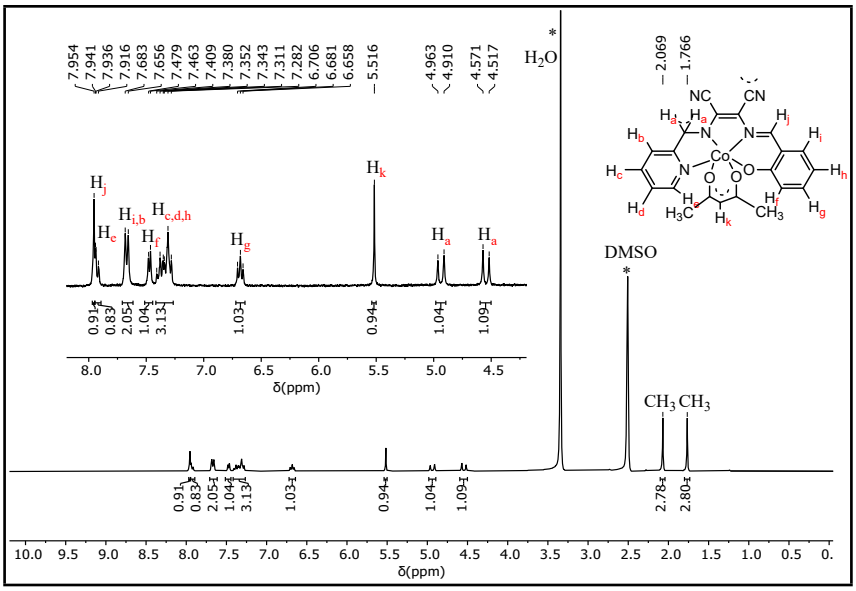

Fig. S7a: ^{1}H NMR Spectrum of **Co-1^{H}** in DMSO-d_6.

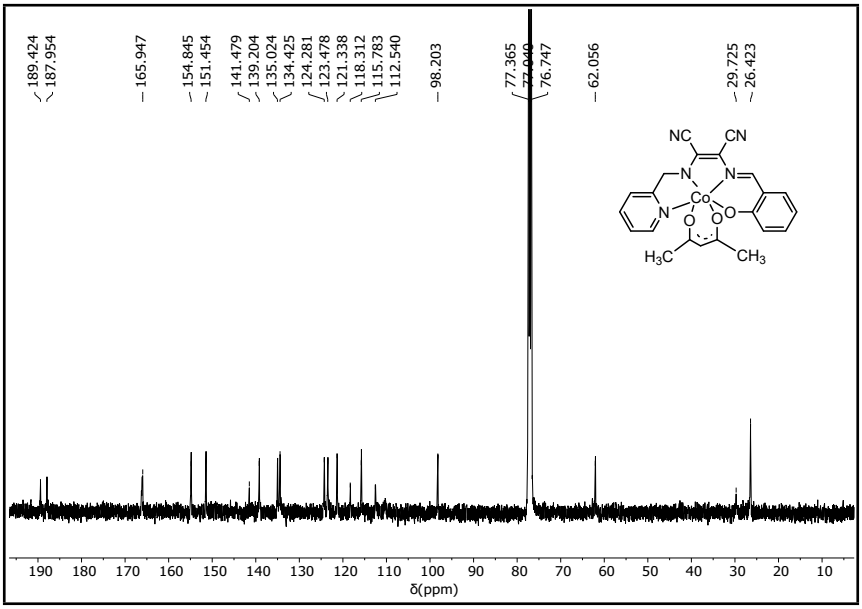

Fig. S8: ^{13}C NMR Spectrum of **Co-1^{H}** in $CDCl_3$.

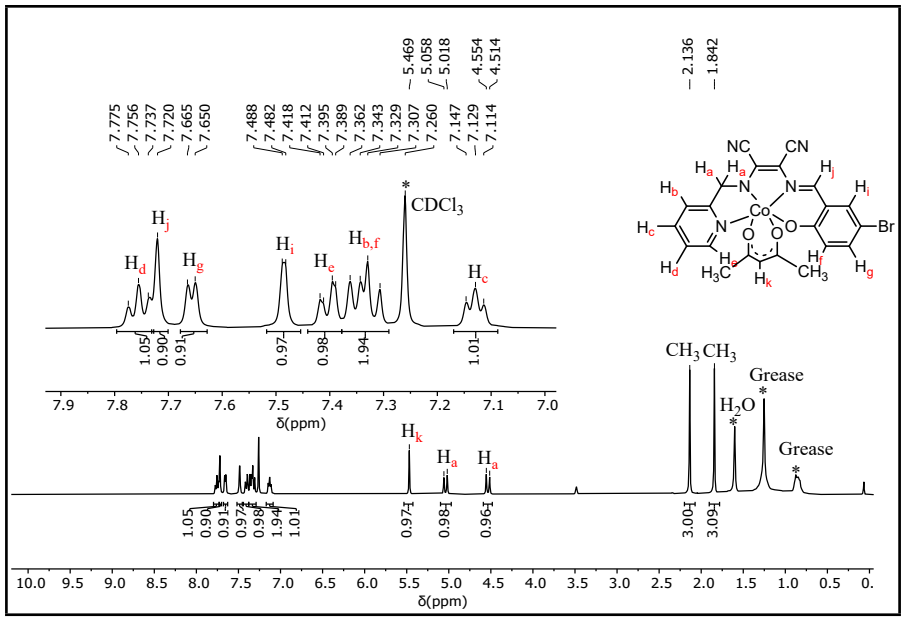

Fig. S9: ^{1}H NMR Spectrum of **Co-1^{Br}** in $CDCl_3$.

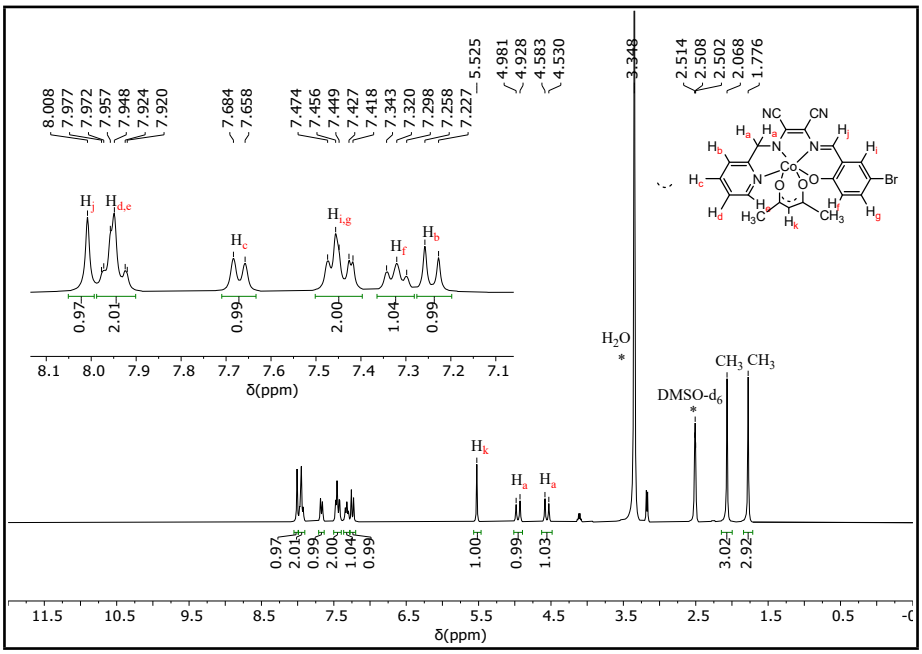

Fig. S9a: ^{1}H NMR Spectrum of **Co-1^{Br}** in DMSO-d_6.

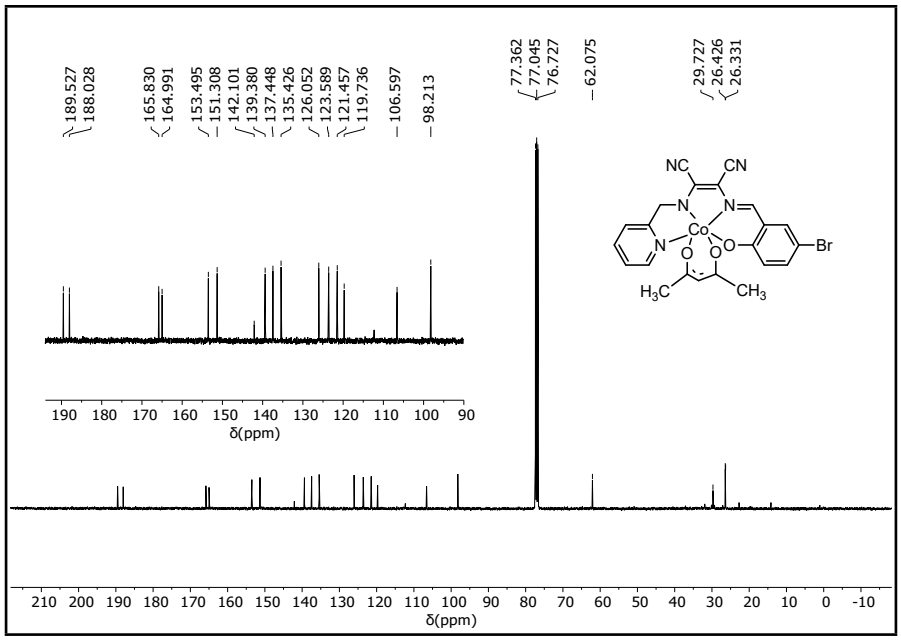

Fig. S10: ^{13}C NMR Spectrum of **Co-1^{Br}** in $CDCl_3$.

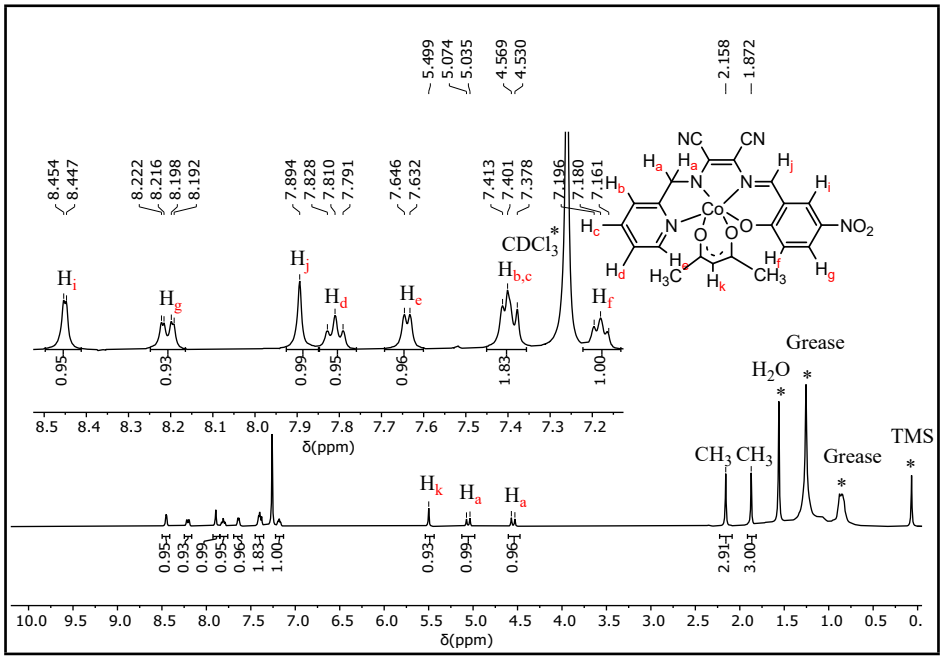

Fig. S11: ^{1}H NMR Spectrum of **Co-1^{NO2}** in $CDCl_3$.

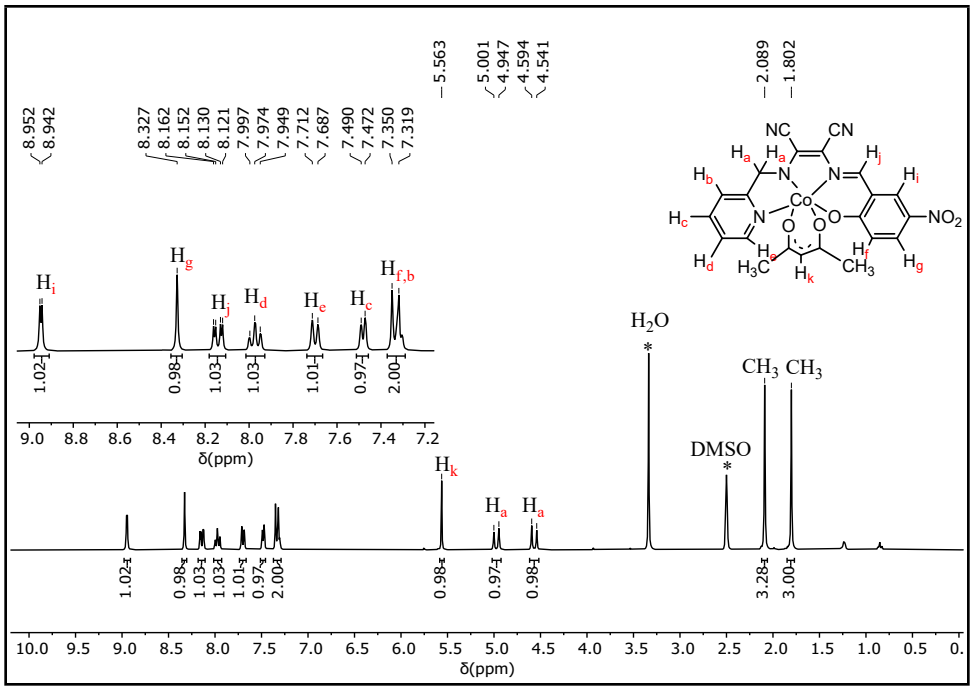

Fig. S11a: ^{1}H NMR Spectrum of **Co-1^{NO2}** in DMSO-d_6.

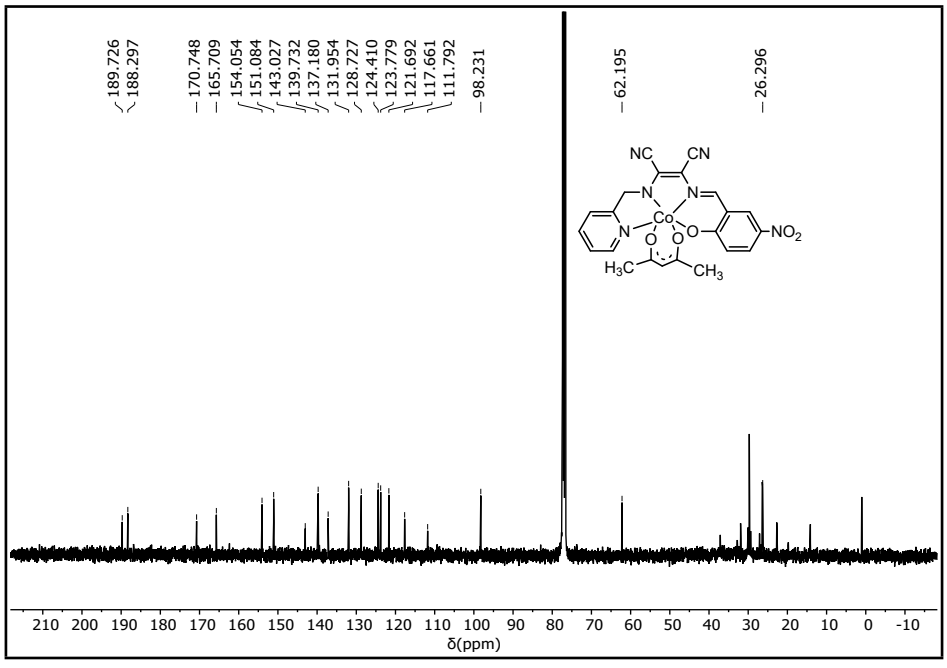

Fig. S12: ^{13}C NMR Spectrum of **Co-1^{NO2}** in $CDCl_3$.

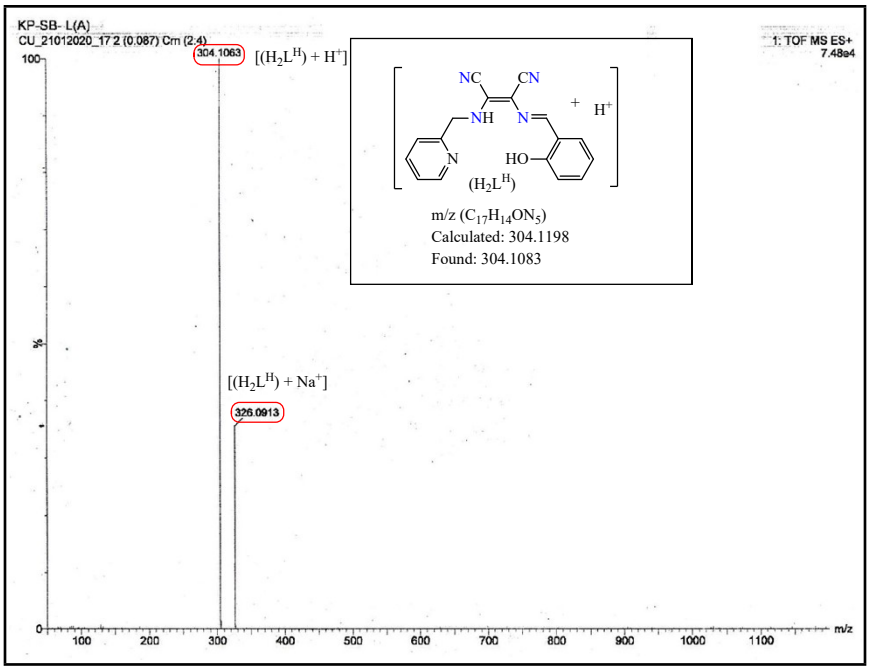

Fig. S13: ESI-MS spectrum of $\mathbf{H_2L^H}$.

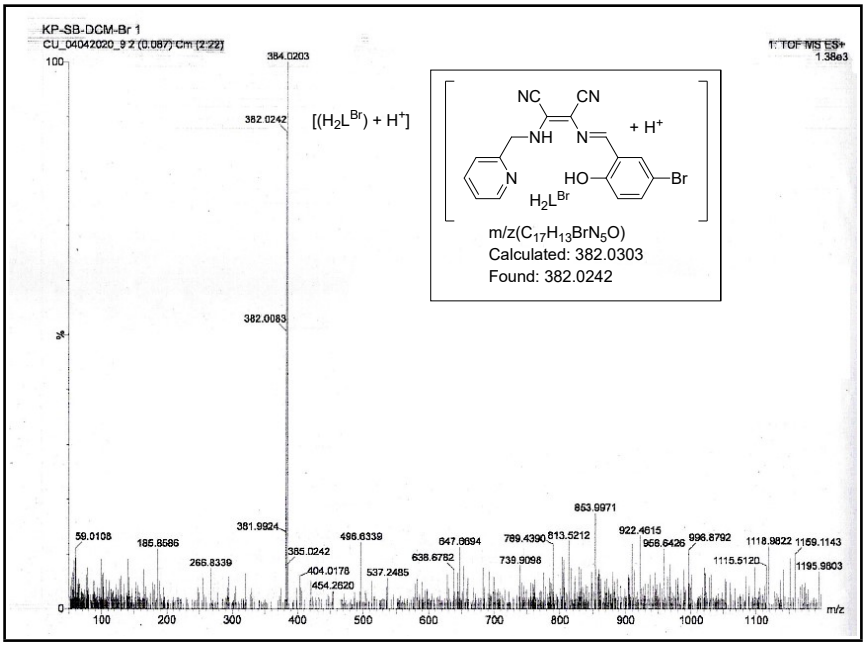

Fig. S14: ESI-MS spectrum of $\mathbf{H_2L^{Br}}$.

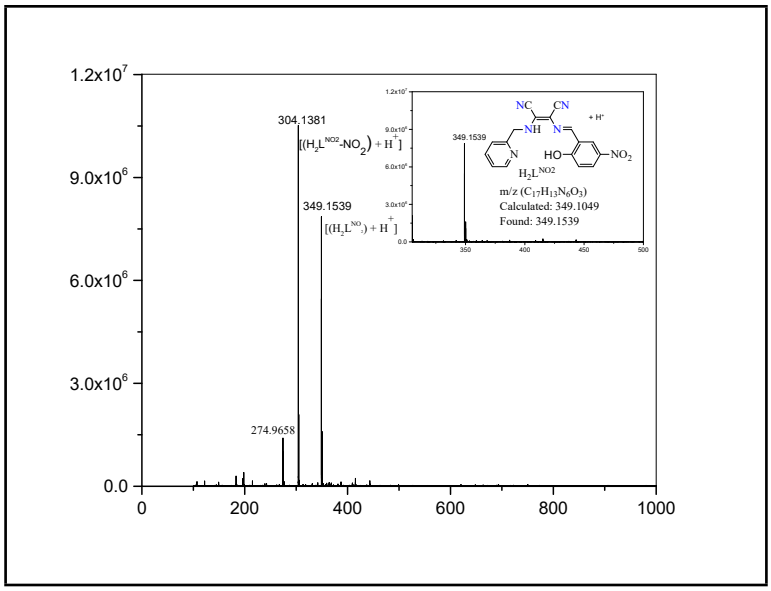

Fig. S15: ESI-MS spectrum of $\mathbf{H_2L^{NO2}}$.

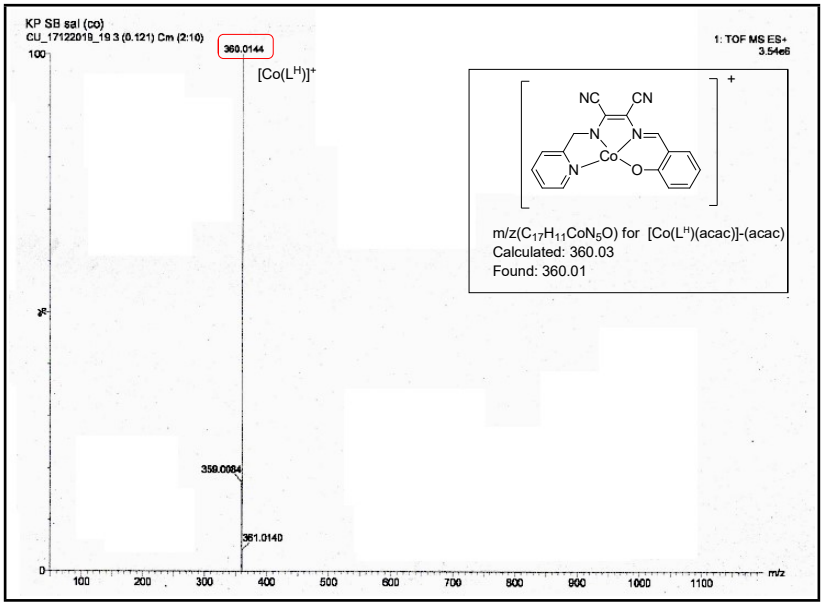

Fig.S16: ESI-MS spectrum of **Co-1^{H}.**

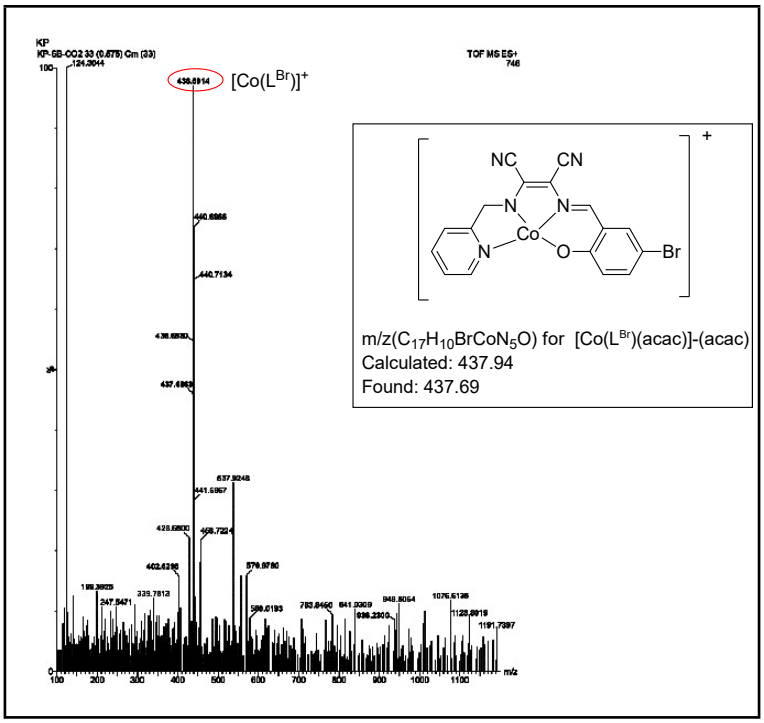

Fig. S17: ESI-MS spectrum of **Co-1^{Br}**.

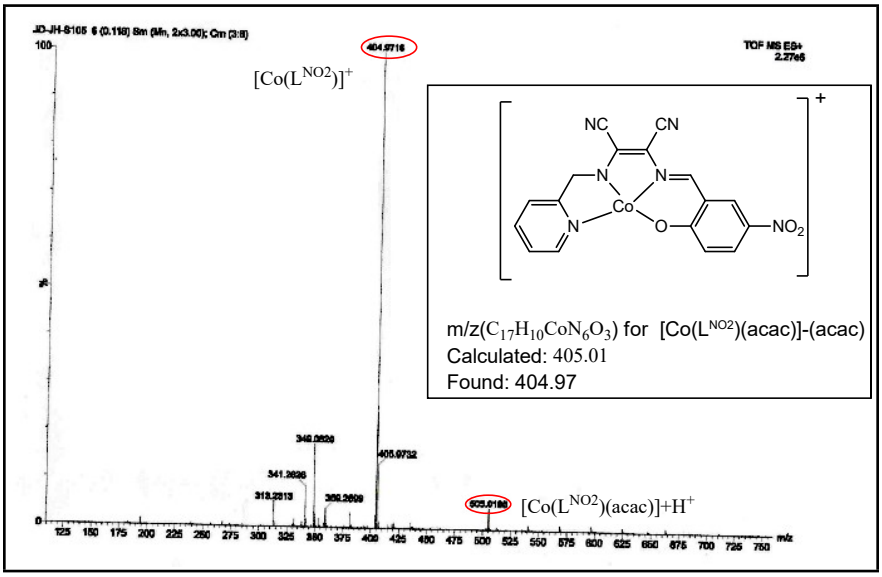

Fig. S18: ESI-MS spectrum of **Co-1^{NO2}**.

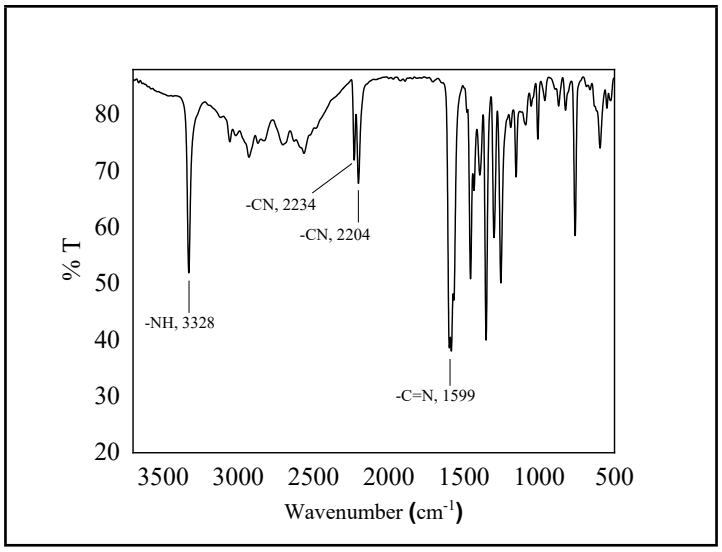

Fig. S19: FTIR spectrum of $\mathbf{H_2L^H}$.

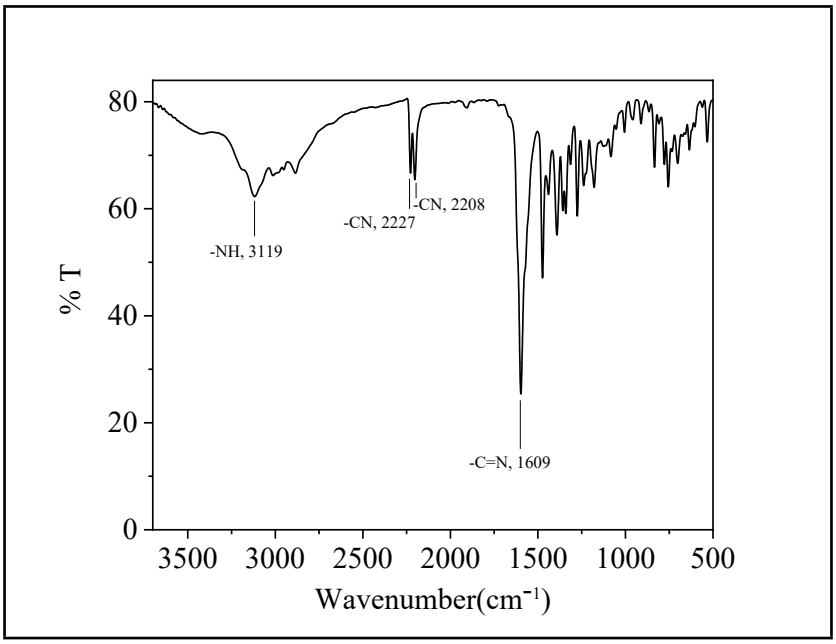

Fig. S20: FTIR spectrum of $\mathbf{H_2L^{Br}}$.

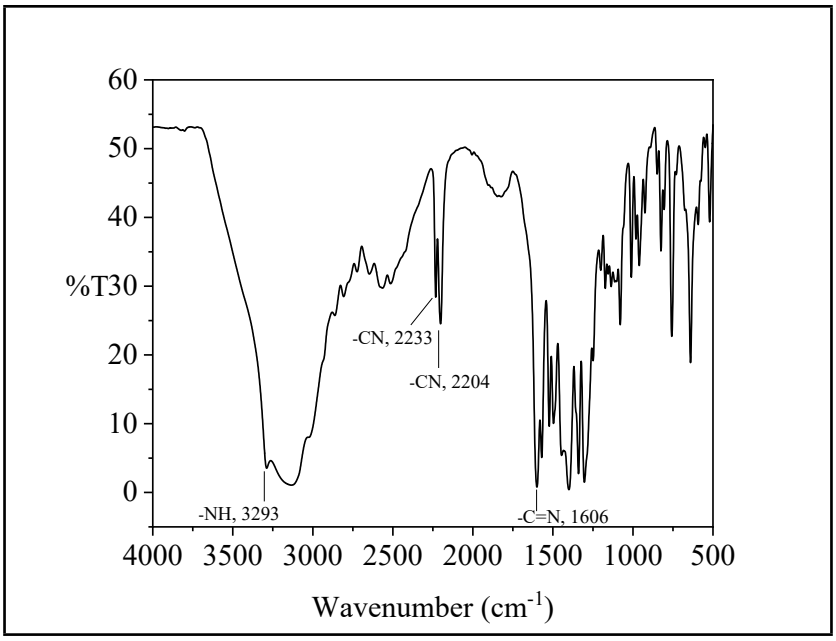

Fig. S21: FTIR spectrum of $\mathbf{H_2L^{NO2}}$.

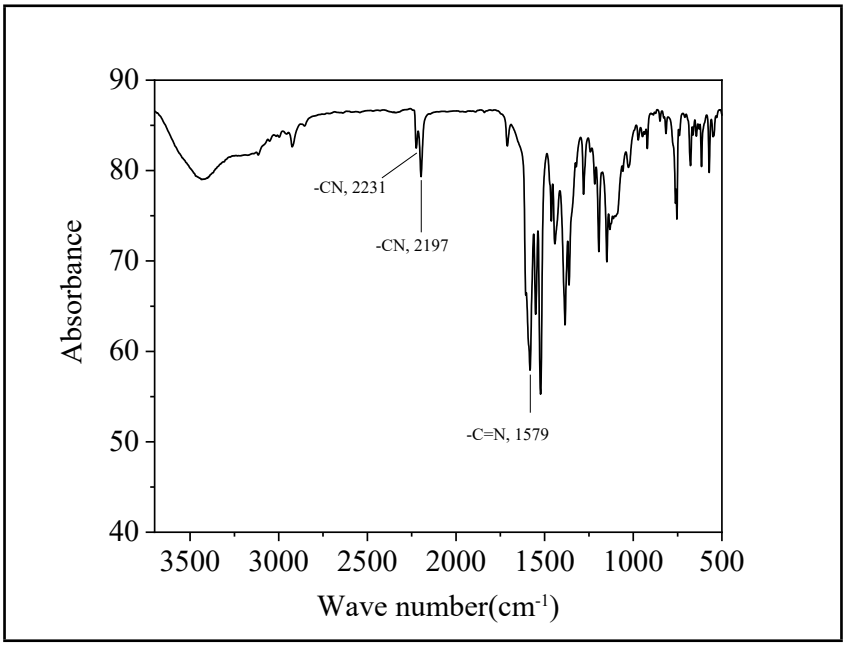

Fig. S22: FTIR spectrum of **Co-1^{H}.**

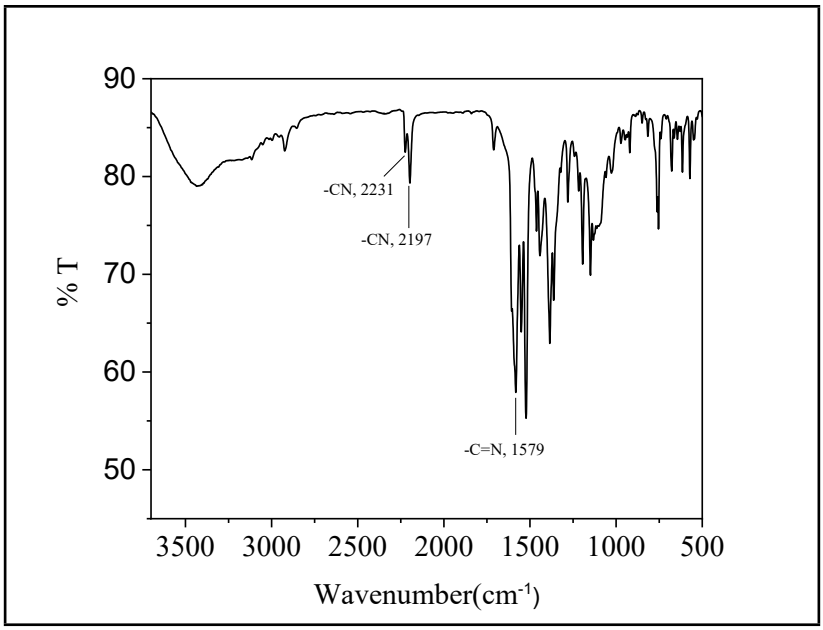

Fig. S23: FTIR spectrum of **Co-1^{Br}.**

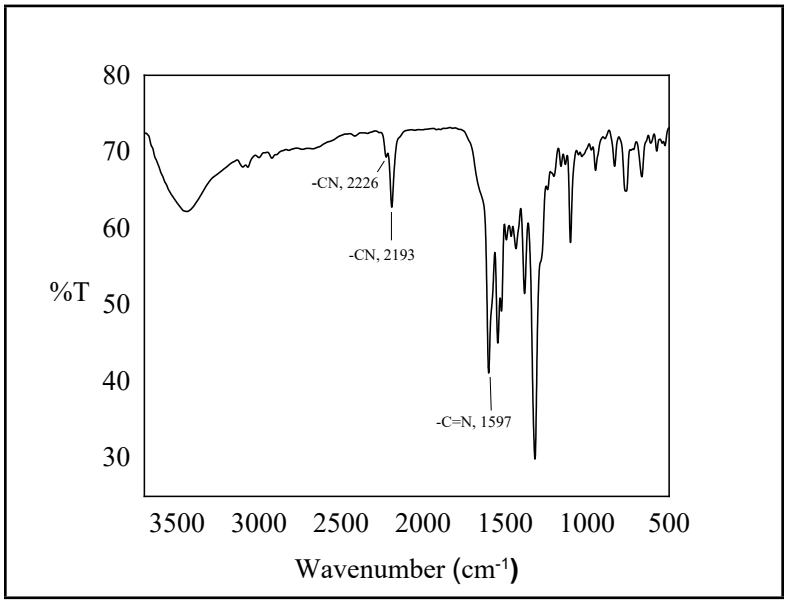

Fig. S24: FTIR spectrum of **Co-1^{NO2}.**

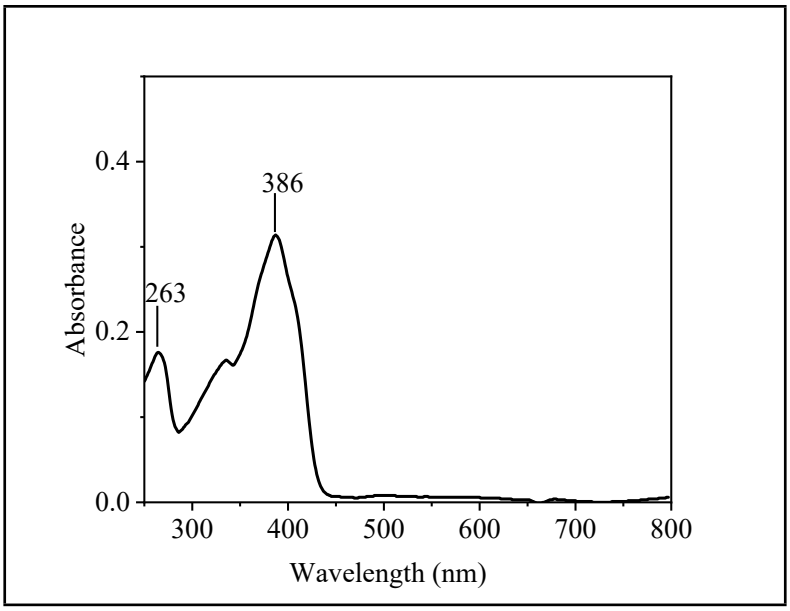

Fig. S25: Electronic absorption spectra of $\mathbf{H_2L^H}$ (0.5 x 10^{-4}(M) in DMF).

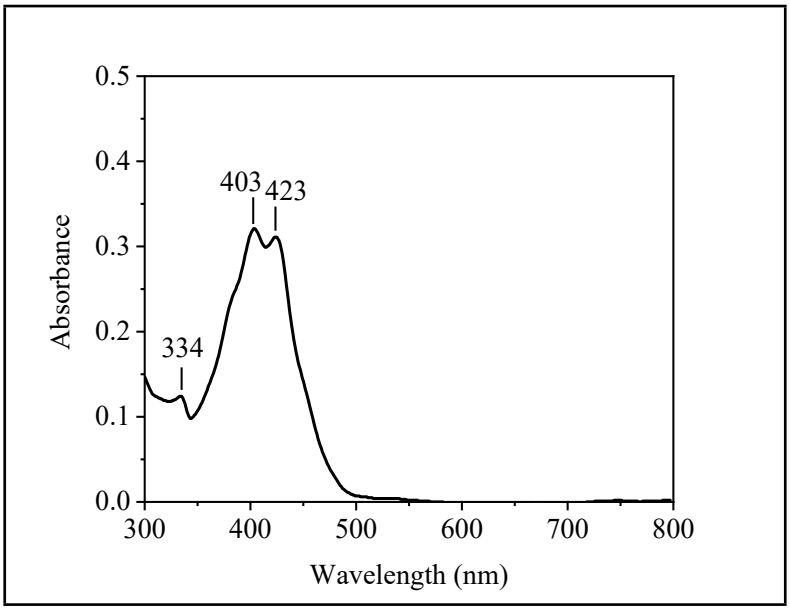

Fig. S26: Electronic absorption spectra of $\mathbf{H_2L^{Br}}$(1 x 10^{-5}(M)) in DMF).

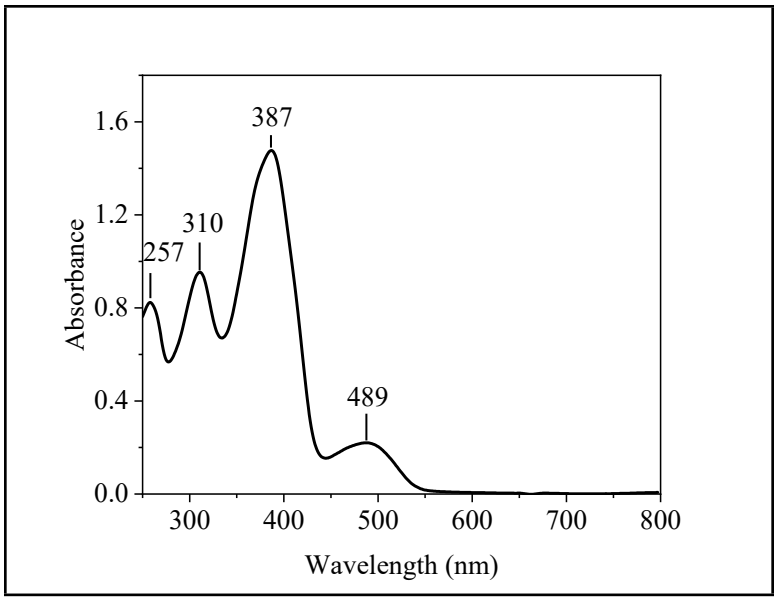

Fig. S27: Electronic absorption spectra of $\mathbf{H_2L^{NO2}}$ (0.5 x 10^{-4}(M) in CH_3CN).

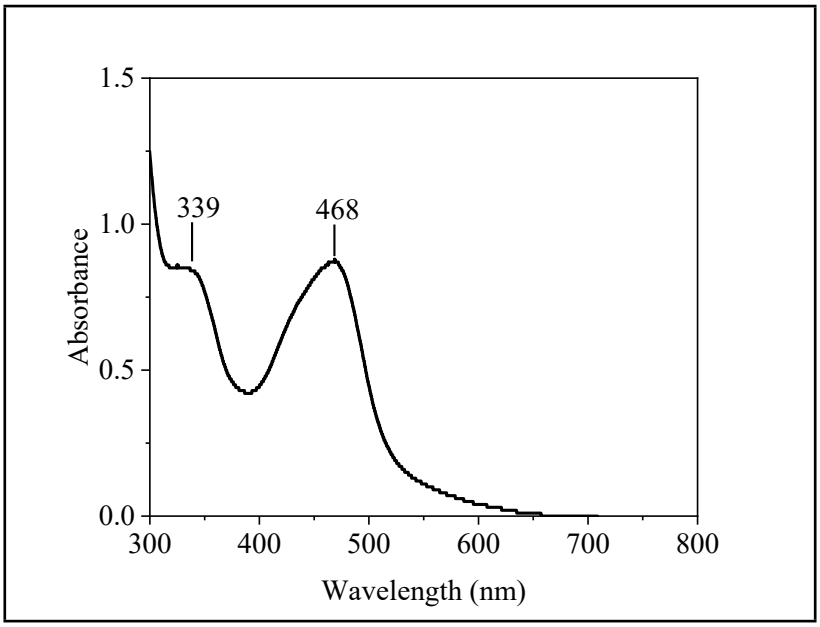

Fig. S28: Electronic absorption spectra of $\mathbf{Co\text{-}1^H}$(0.5 x 10^{-4}(M) in CH_3CN).

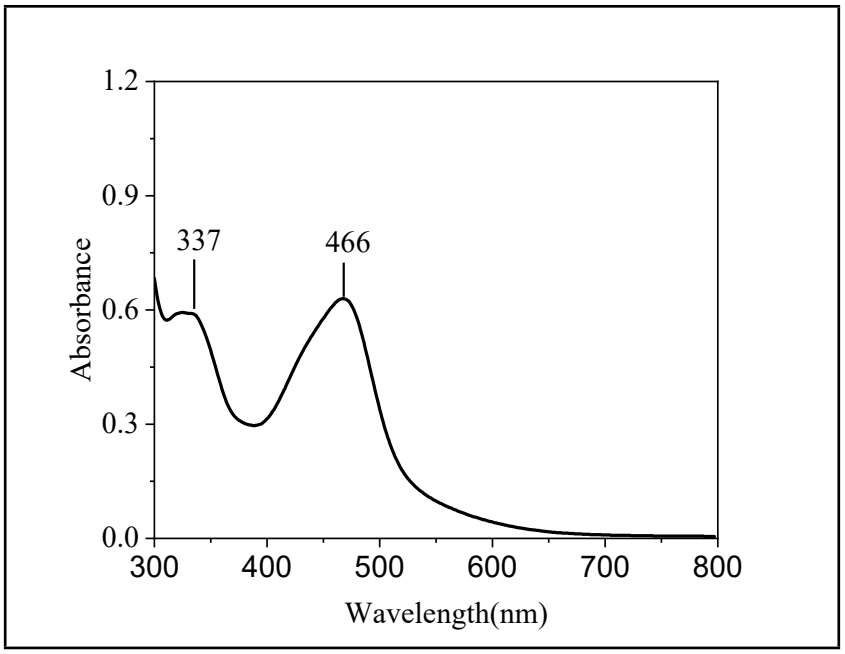

Fig. S29: Electronic absorption spectra of **Co-1^{Br}**(0.5 x 10^{-4}(M) in CH_3CN).

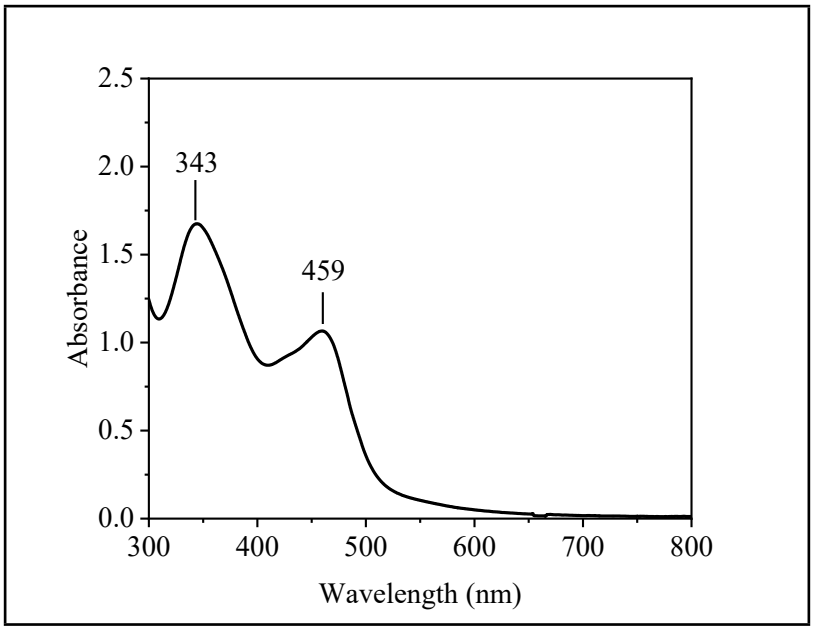

Fig. S30: Electronic absorption spectra of **Co-1^{NO2}**(0.5 x 10^{-4}(M) in CH_3CN).

Hirshfeld Surface Analysis:

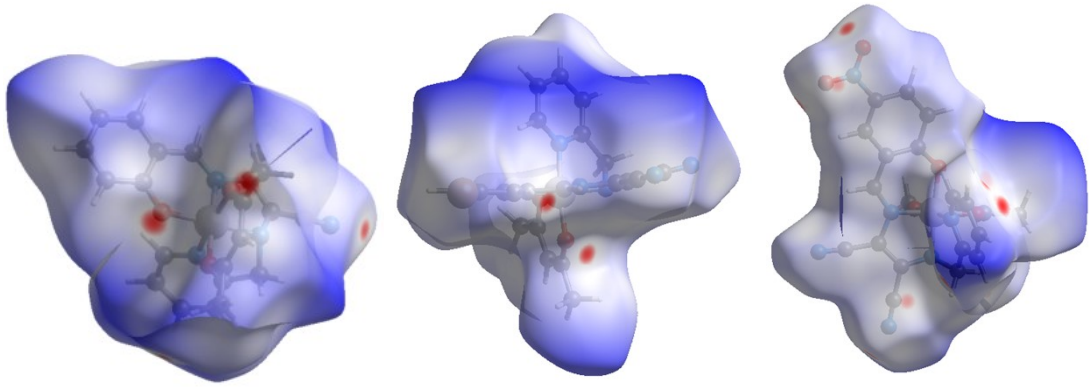

Fig. S31: The d_{norm} of 3D Hirshfeld surfaces of the complex **Co-1^{H}**(left)**, Co-1^{Br}**(middle)and**Co-1^{NO2}**(right)**.**

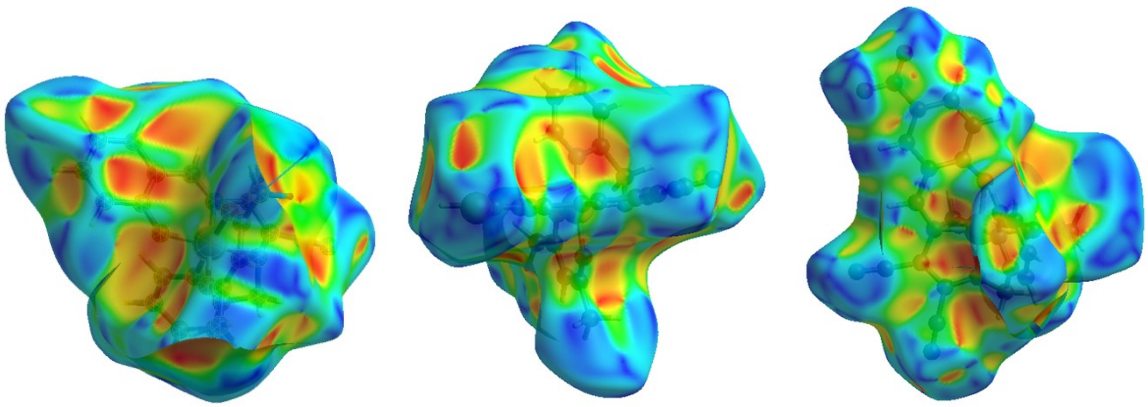

Fig. S32: The shape index of 3D Hirshfeld surfaces of the complex**Co-1^{H}**(left)**, Co-1^{Br}**(middle)and**Co-1^{NO2}**(right)**.**

.

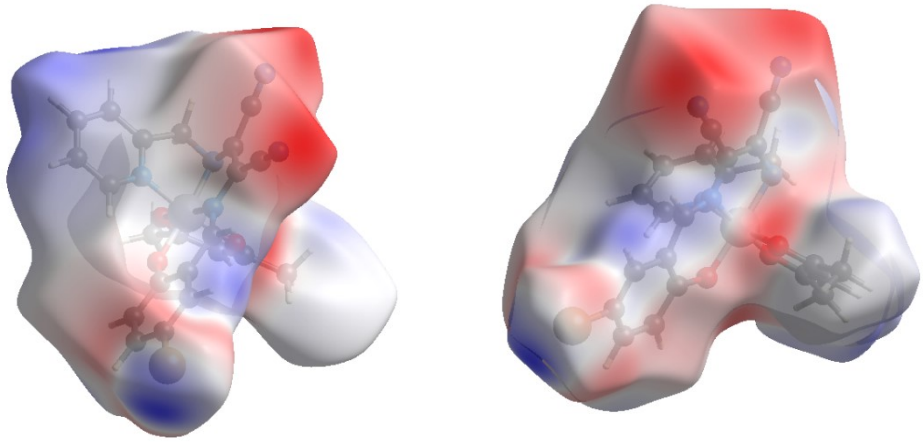

Fig. S33: Two views of three dimensional HS plotted over electrostatic potential for **Co-1^{Br}**.

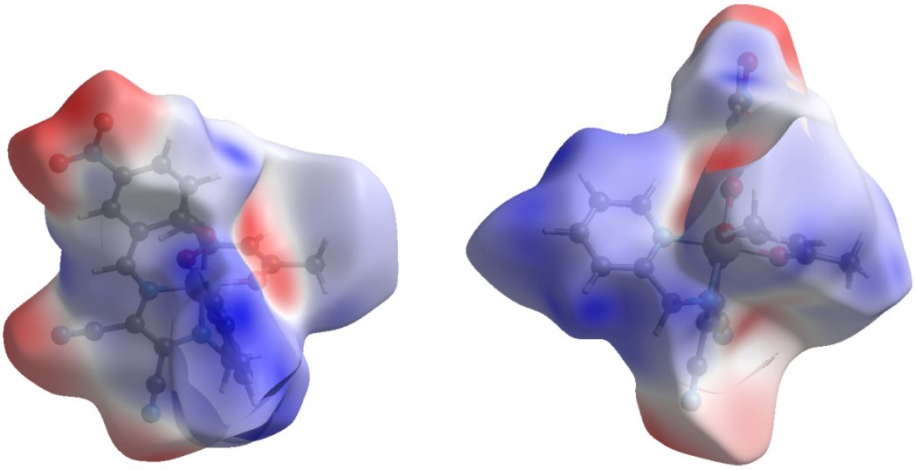

Fig. S34: Two views of three dimensional HS plotted over electrostatic potential for **Co-1^{NO2}**.

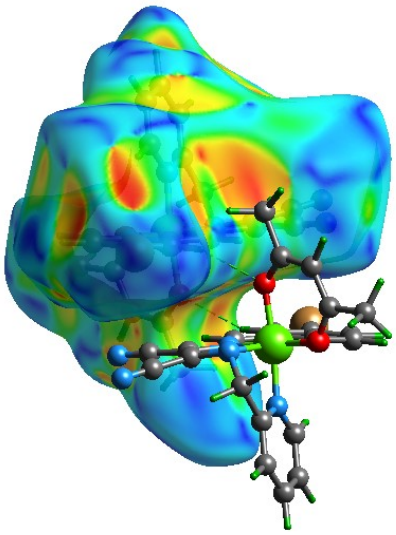

Fig. S35: Three dimensional HS plotted shape index along with representative interacting molecules in surface for **Co-1^{Br}**.

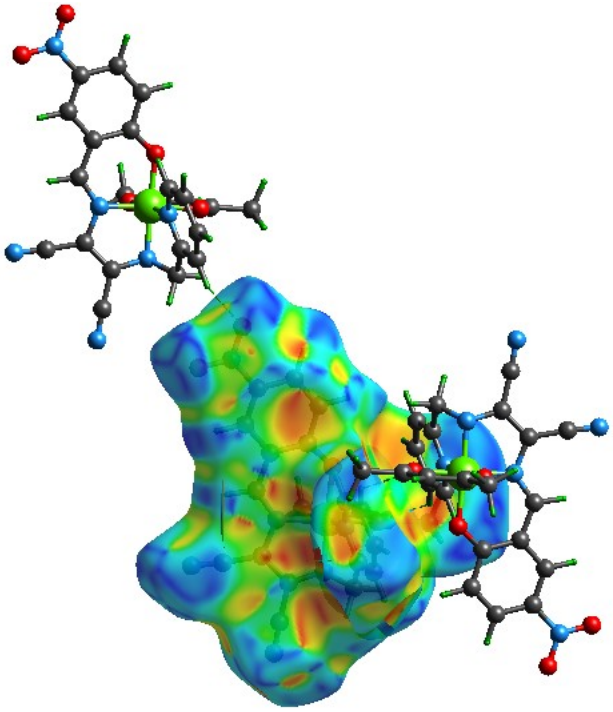

Fig. S36: Three dimensional HS plotted shape index along with representative interacting molecules in surface for **Co-1^{NO2}**.

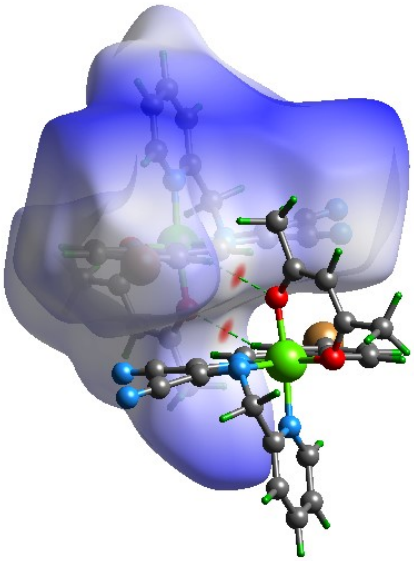

Fig. S37: Three dimensional HS plotted over d_{norm} along with representative interacting molecules in surface for **Co-1^{Br}**.

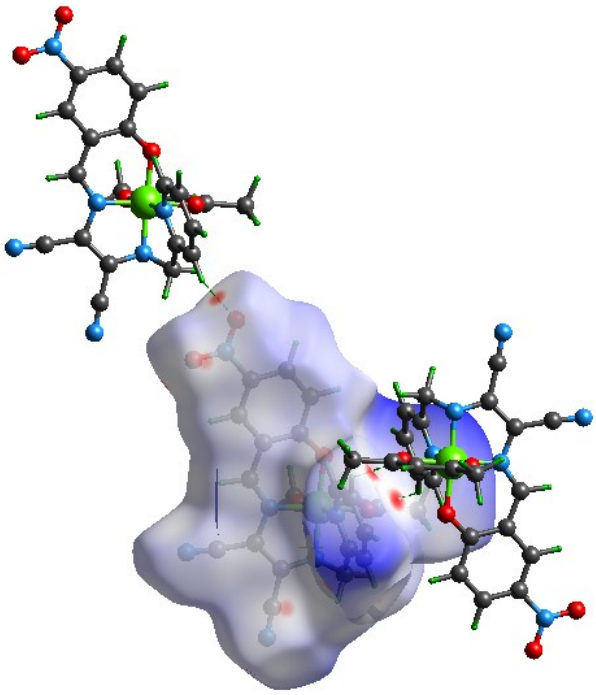

Fig. S38: Three dimensional HS plotted over d_{norm} along with representative interacting molecules in surface for **Co-1^{NO2}**.

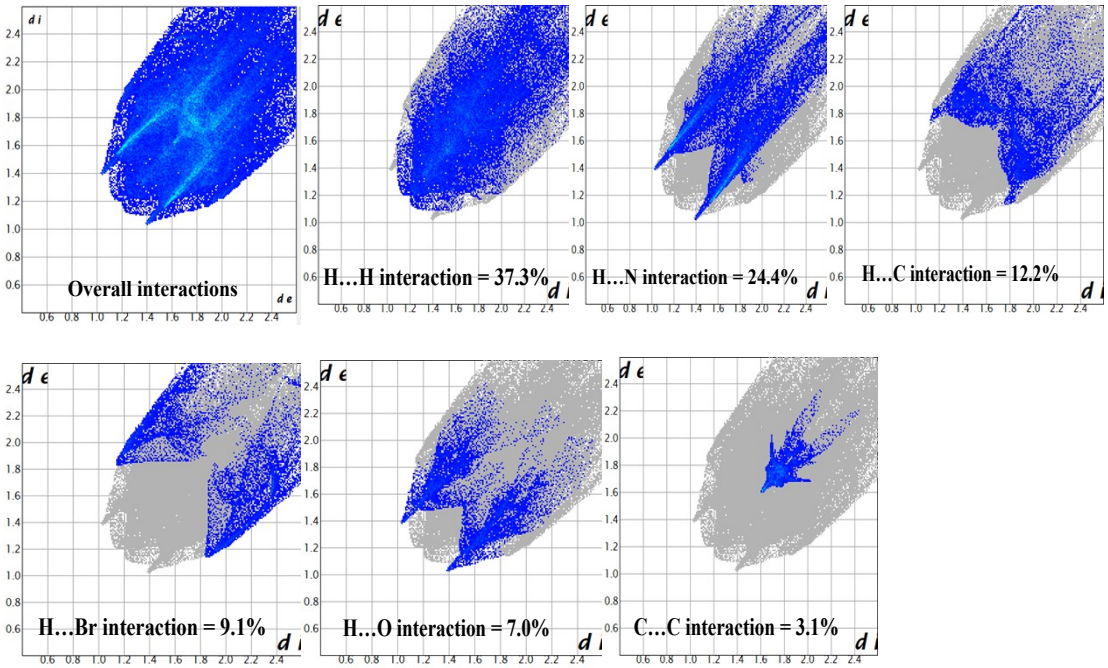

Fig. S39:2D Fingerprint plots as obtained from the crystal structures for different type of interactions (a) Overall, (b)H..H, (c) H..N, (d) H..C, (e) H..Br, (f) H..O and (g) C..C present in the complex, **Co-1^{Br}**. The term 'd_i' stands for distance from the HS to the nearest atom inside the HS, whereas de stands for the same from to the nearest atom outside the HS.

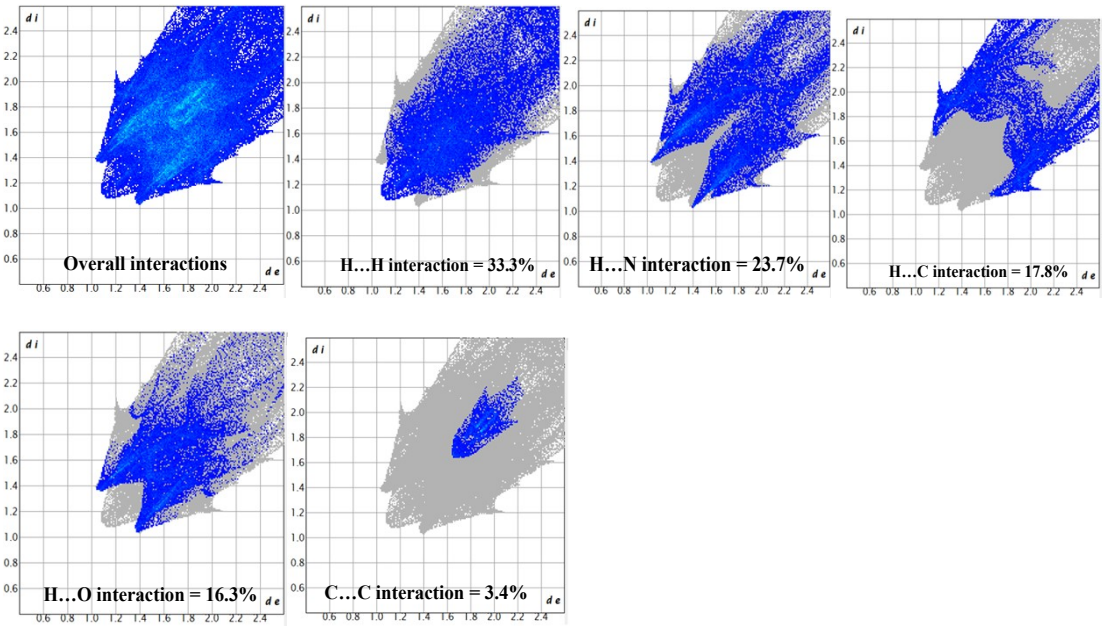

Fig. S40:2D Fingerprint plots as obtained from the crystal structures for different type of interactions (a) Overall, (b)H..H, (c) H..N, (d) H..C, (e) H..O, and (f) C..C present in the complex, **Co-1^{NO2}**. The term 'd_i' stands for distance from the HS to the nearest atom inside the HS, whereas de stands for the same from to the nearest atom outside the HS.

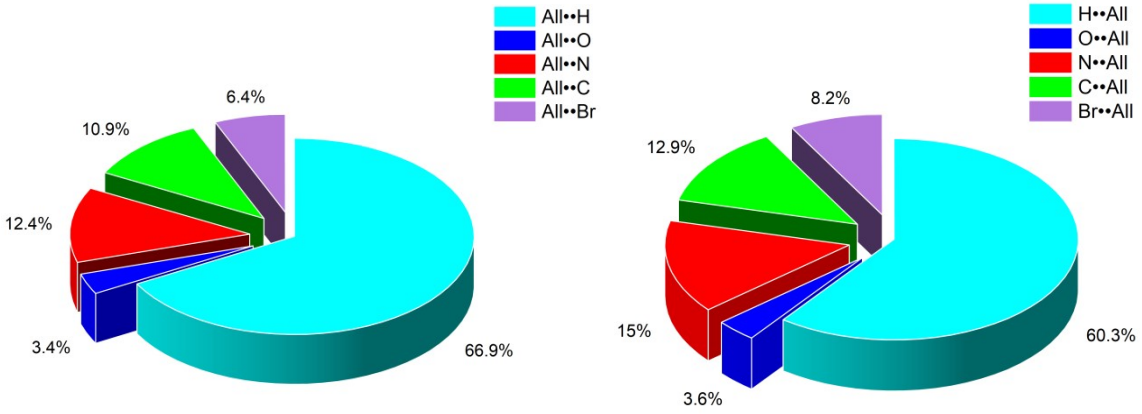

Fig. S41: Left: Percentage contributions of the interaction of all the atoms present inside the HS to an atom outside the HS. Right: Percentage contributions of the interaction of an atom present inside the HS to all the atoms present in the surrounding of the HS for complex **Co-1^{Br}**.

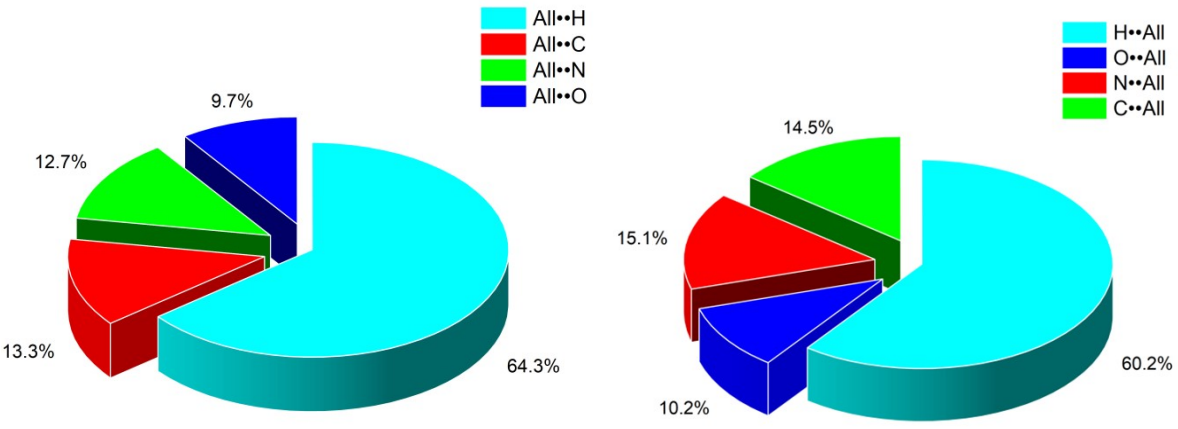

Fig. S42: Left: Percentage contributions of the interaction of all the atoms present inside the HS to an atom outside the HS. Right: Percentage contributions of the interaction of an atom present inside the HS to all the atoms present in the surrounding of the HS for complex **Co-1^{NO2}**.

Interaction Energies (kJ/mol)
R is the distance between molecular centroids (mean atomic position) in Å.

Total energies, only reported for two benchmarked energy models, are the sum of the four energy components, scaled appropriately (see the scale factor table below)

	N	Symop	R	Electron Density	E_ele	E_pol	E_dis	E_rep	E_tot
	2	x, y, z	8.87	B3LYP/6-31G(d,p)	-13.9	-4.9	-32.5	21.4	-33.4
	2	x, y, z	10.51	B3LYP/6-31G(d,p)	0.3	-1.1	-21.1	11.5	-11.8
	2	x, y, z	10.28	B3LYP/6-31G(d,p)	-13.4	-2.9	-8.6	10.2	-17.5
	1	-x, -y, -z	7.61	B3LYP/6-31G(d,p)	-7.4	-6.6	-52.9	27.9	-41.6
	1	-x, -y, -z	8.67	B3LYP/6-31G(d,p)	-39.6	-13.5	-49.7	41.0	-69.8
	1	-x, -y, -z	7.98	B3LYP/6-31G(d,p)	-25.8	-6.8	-60.6	44.4	-57.7
	1	-x, -y, -z	10.62	B3LYP/6-31G(d,p)	-9.6	-4.3	-8.3	3.1	-18.7
	1	-x, -y, -z	12.56	B3LYP/6-31G(d,p)	5.6	-1.4	-4.8	0.0	0.7
	1	-x, -y, -z	12.31	B3LYP/6-31G(d,p)	1.1	-0.3	-5.4	0.0	-3.8
	1	-x, -y, -z	11.45	B3LYP/6-31G(d,p)	-1.6	-0.3	-4.1	0.1	-5.4

Scale factors for benchmarked energy models
See Mackenzie et al. IUCrJ (2017)

Energy Model	k_ele	k_pol	k_disp	k_rep
CE-HF ... HF/3-21G electron densities	1.019	0.651	0.901	0.811
CE-B3LYP ... B3LYP/6-31G(d,p) electron densities	1.057	0.740	0.871	0.618

Fig. S43. Interaction energies for the complex **Co-1^{H}.**

Interaction Energies (kJ/mol)
R is the distance between molecular centroids (mean atomic position) in Å.

Total energies, only reported for two benchmarked energy models, are the sum of the four energy components, scaled appropriately (see the scale factor table below)

	N	Symop	R	Electron Density	E_ele	E_pol	E_dis	E_rep	E_tot
	2	x, y, z	12.26	B3LYP/6-31G(d,p)	-13.0	-1.2	-19.6	0.0	-31.7
	2	x, y, z	11.37	B3LYP/6-31G(d,p)	-2.7	-2.2	-8.7	5.8	-8.5
	1	-x, -y, -z	11.39	B3LYP/6-31G(d,p)	-2.4	-0.4	-9.3	1.7	-9.9
	1	-x, -y, -z	8.82	B3LYP/6-31G(d,p)	-14.0	-3.7	-49.1	26.0	-44.3
	2	x, y, z	12.11	B3LYP/6-31G(d,p)	-3.5	-2.1	-5.6	0.0	-10.2
	1	-x, -y, -z	10.76	B3LYP/6-31G(d,p)	-13.0	-3.6	-18.7	10.3	-26.3
	2	x, y, z	11.48	B3LYP/6-31G(d,p)	3.4	-1.4	-9.6	5.4	-2.5
	1	-x, -y, -z	8.85	B3LYP/6-31G(d,p)	-23.9	-8.8	-65.6	54.1	-55.4
	1	-x, -y, -z	5.89	B3LYP/6-31G(d,p)	-27.3	-5.5	-99.5	80.5	-69.8
	1	-x, -y, -z	12.55	B3LYP/6-31G(d,p)	-29.1	-6.6	-12.1	0.0	-46.2

Scale factors for benchmarked energy models
See Mackenzie et al. IUCrJ (2017)

Energy Model	k_ele	k_pol	k_disp	k_rep
CE-HF ... HF/3-21G electron densities	1.019	0.651	0.901	0.811
CE-B3LYP ... B3LYP/6-31G(d,p) electron densities	1.057	0.740	0.871	0.618

Fig. S44. Interaction energies for the complex **Co-1^{Br}.**

Interaction Energies (kJ/mol)
R is the distance between molecular centroids (mean atomic position) in Å.

Total energies, only reported for two benchmarked energy models, are the sum of the four energy components, scaled appropriately (see the scale factor table below)

	N	Symop	R	Electron Density	E_ele	E_pol	E_dis	E_rep	E_tot
	1	-x, -y, -z	5.88	B3LYP/6-31G(d,p)	-39.3	-17.8	-113.5	79.9	-104.3
	1	-x, -y, -z	16.12	B3LYP/6-31G(d,p)	10.1	-1.0	-1.8	0.0	8.3
	2	x, y, z	12.92	B3LYP/6-31G(d,p)	-5.2	-5.2	-13.2	0.0	-20.8
	1	x, y, z	11.90	B3LYP/6-31G(d,p)	1.0	-2.9	-9.8	12.3	-2.0
	1	-x, -y, -z	11.96	B3LYP/6-31G(d,p)	-21.8	-4.4	-9.7	6.0	-31.0
	0	-x, -y, -z	9.32	B3LYP/6-31G(d,p)	-13.5	-2.2	-26.2	19.5	-26.6
	0	-x, -y, -z	9.82	B3LYP/6-31G(d,p)	-10.5	-2.3	-14.0	7.4	-20.4
	0	-x, -y, -z	9.33	B3LYP/6-31G(d,p)	-10.7	-4.5	-59.3	39.6	-41.8
	1	-x, -y, -z	12.48	B3LYP/6-31G(d,p)	-8.5	-1.9	-7.8	0.0	-17.2
	1	x, y, z	10.28	B3LYP/6-31G(d,p)	-6.5	-1.9	-8.4	2.2	-14.2
	1	-x, -y, -z	7.84	B3LYP/6-31G(d,p)	-25.1	-11.4	-71.8	66.6	-56.4

Scale factors for benchmarked energy models
See Mackenzie et al. IUCrJ (2017)

Energy Model	k_ele	k_pol	k_disp	k_rep
CE-HF ... HF/3-21G electron densities	1.019	0.651	0.901	0.811
CE-B3LYP ... B3LYP/6-31G(d,p) electron densities	1.057	0.740	0.871	0.618

Fig. S45. Interaction energies for the complex **Co-1^{NO2}.**

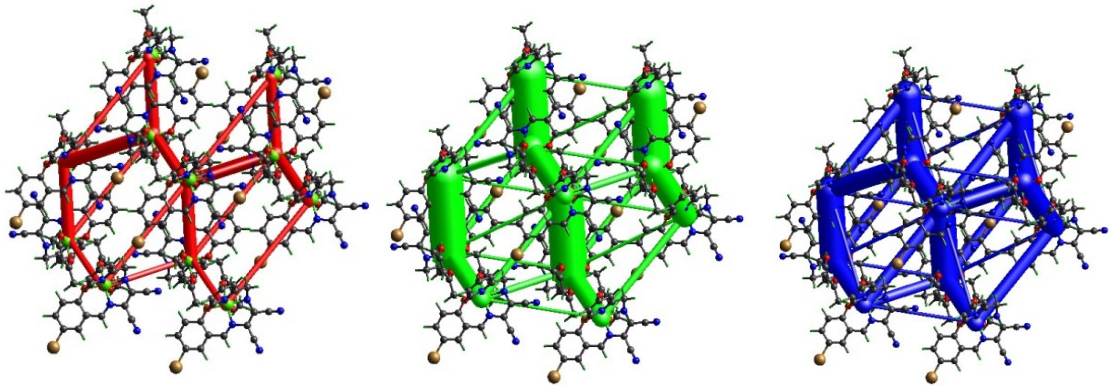

Fig. S46: Energy framework diagramfor **Co-1^{Br}**(Left: Coulomb Energy, Middle: Dispersion Energy, Right: Total Energy) for **Co-1^{Br}**. Scale factor of 50 kJ mol-1 with a cut-off value of 5 kJ mol^{-1}.

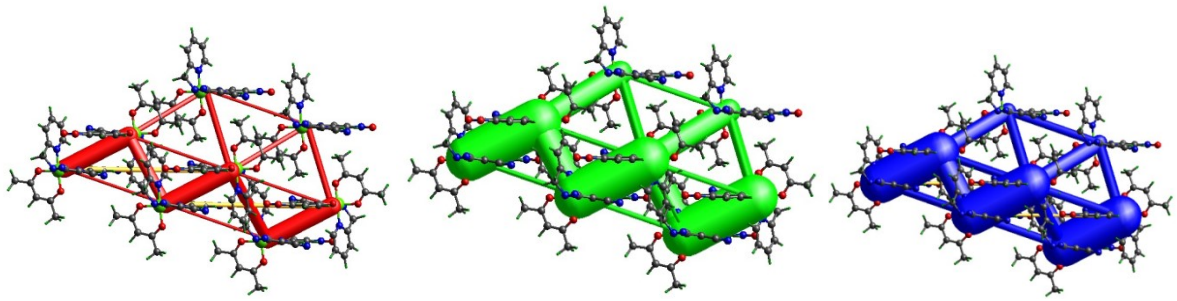

Fig. S47: Energy framework diagramfor **Co-1^{NO2}**(Left: Coulomb Energy, Middle: Dispersion Energy, Right: Total Energy) for **Co-1^{NO2}**. Scale factor of 50 kJ mol-1 with a cut-off value of 5 kJ mol^{-1}.

Catalytic Study:

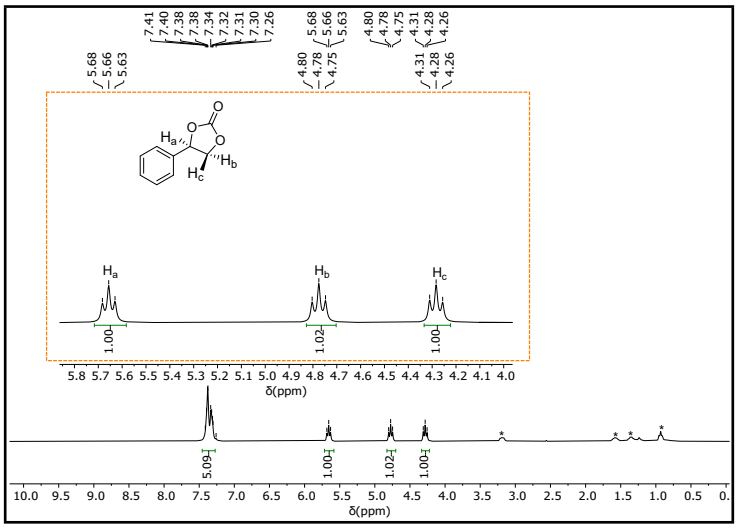

Fig. S48:^{1}H NMR Spectrum in $CDCl_3$ obtained for a reaction mixture taken after 22 hrs (**Co-1^{H}**: 1.5 mol%, TBAB: 5 mol%) showing three peaks of styrene carbonate (>99% conversion) [* indicates Tetrabutyl ammonium bromide (TBAB) peaks].

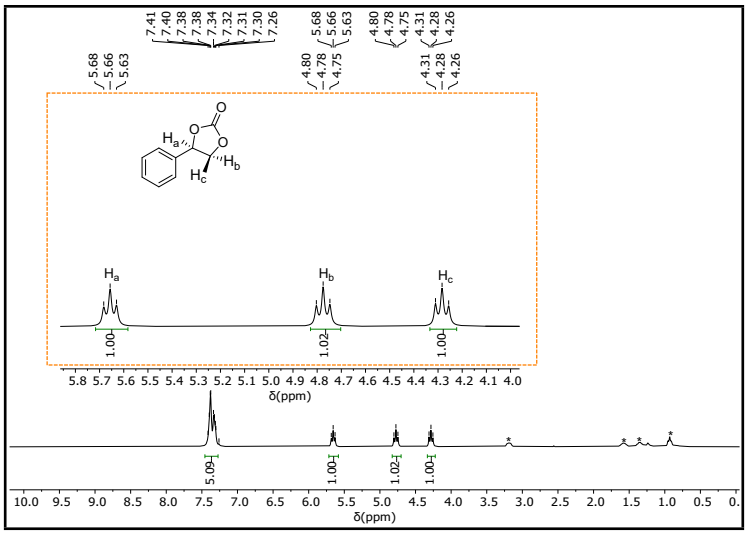

Fig. S49: ^{1}H NMR Spectrum in $CDCl_3$ obtained for a reaction mixture taken after 22 hrs (**Co-1^{Br}**: 1.5 mol%, TBAB: 5 mol%) showing three peaks of styrene carbonate (>99% conversion) [* indicates Tetrabutyl ammonium bromide (TBAB) peaks].

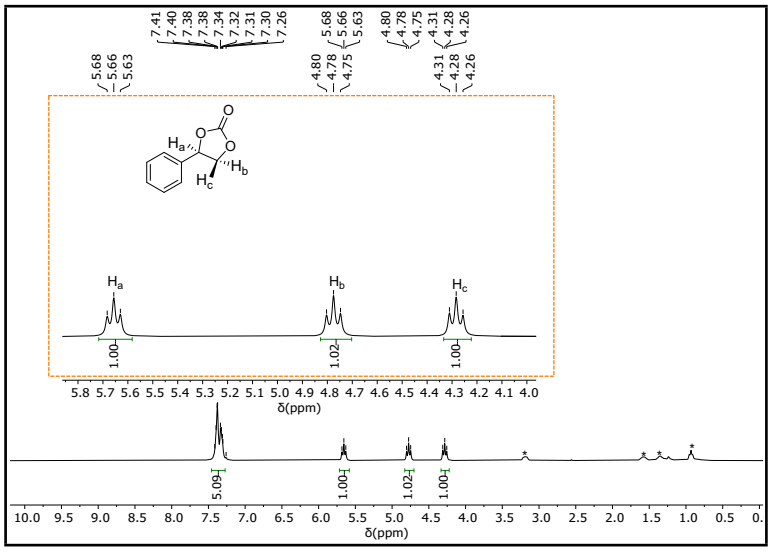

Fig. S50: ^{1}H NMR Spectrum in $CDCl_3$ obtained for a reaction mixture taken after 22 hrs (**Co-1^{NO2}**: 1.5 mol%, TBAB: 5 mol%) showing three peaks of styrene carbonate (>99% conversion) [* indicates Tetrabutyl ammonium bromide (TBAB) peaks].

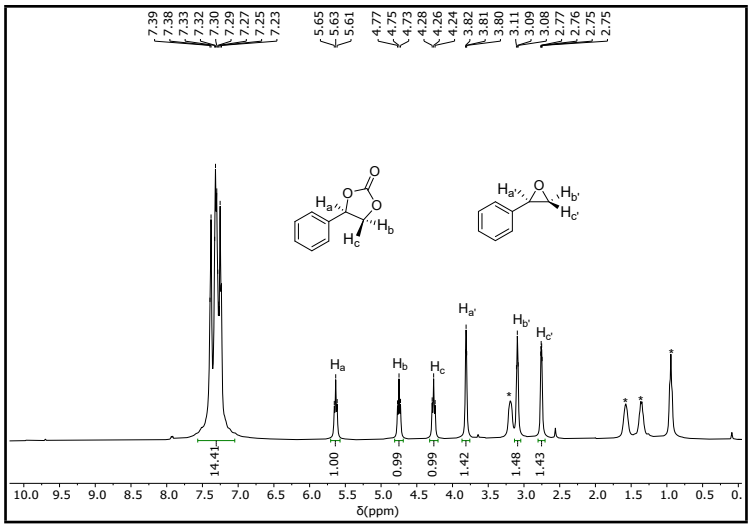

Fig. S51: ^{1}H NMR Spectrum in $CDCl_3$ obtained for a reaction mixture taken after 8 hrs (**Co-1^{H}**: 1.5 mol%, TBAB: 5 mol%) showing three peaks of styrene carbonate and three peaks associated to styrene oxide starting material (41% conversion) [* indicates Tetrabutyl ammonium bromide (TBAB) peaks].

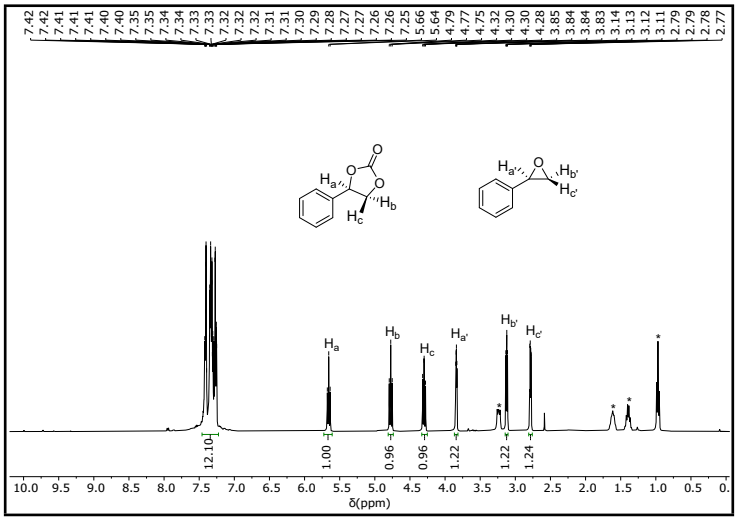

Fig. S52: ^{1}H NMR Spectrum in $CDCl_3$ obtained for a reaction mixture taken after 8 hrs (**Co-1^{Br}**: 1.5 mol%, TBAB: 5 mol%) showing three peaks of styrene carbonate and three peaks associated to styrene oxide starting material (45% conversion) [* indicates Tetrabutyl ammonium bromide (TBAB) peaks].

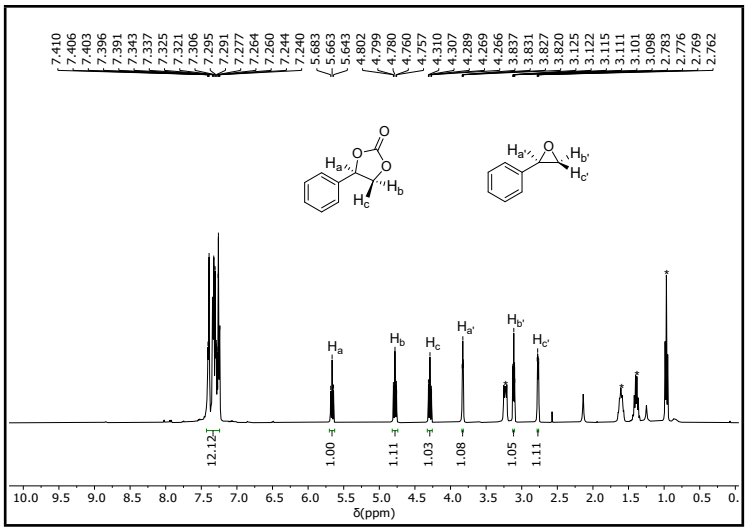

Fig. S53: ^{1}H NMR Spectrum in $CDCl_3$ obtained for a reaction mixture taken after 8 hrs (**Co-1^{NO2}**: 1.5 mol%, TBAB: 5 mol%) showing three peaks of styrene carbonate and three peaks associated to styrene oxide starting material (48% conversion) [* indicates Tetrabutyl ammonium bromide (TBAB) peaks].

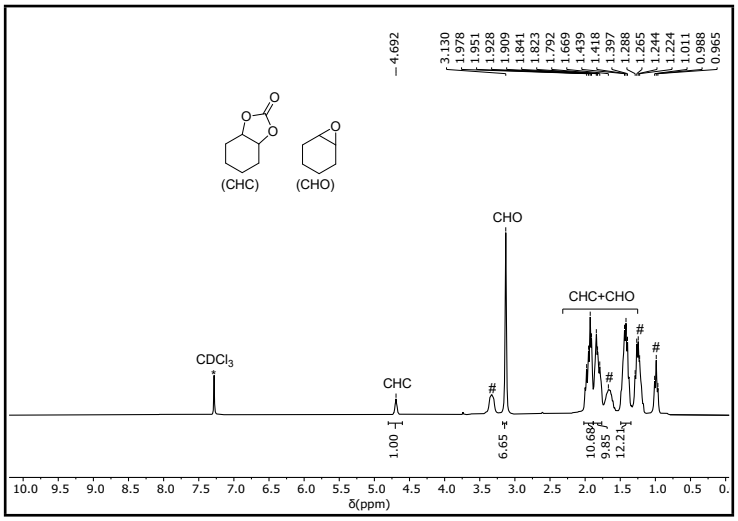

Fig. S54: ^{1}H NMR Spectrum in $CDCl_3$ obtained for a reaction mixture taken after 22 hrs (**Co-1^{H}**: 1.5 mol%, TBAB: 5 mol%) showing peaks of cyclohexane carbonate (13% conversion) at room temperature. [# indicates Tetrabutyl ammonium bromide (TBAB) peaks].

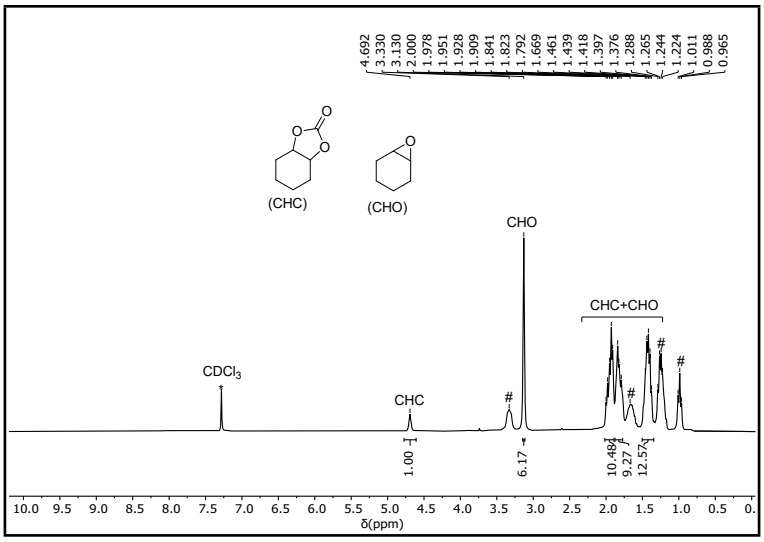

Fig. S55: ^{1}H NMR Spectrum in $CDCl_3$ obtained for a reaction mixture taken after 22 hrs (**Co-1^{Br}**: 1.5 mol%, TBAB: 5 mol%) showing peaks of cyclohexane carbonate (15% conversion) at room temperature. [# indicates Tetrabutyl ammonium bromide (TBAB) peaks].

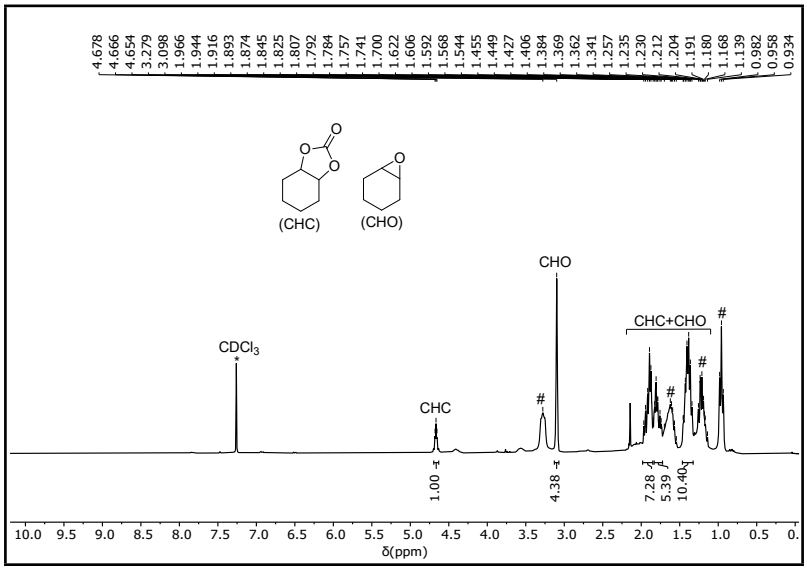

Fig. S56: ^{1}H NMR Spectrum in $CDCl_3$ obtained for a reaction mixture taken after 22 hrs (**Co-1^{NO2}**: 1.5 mol%, TBAB: 5 mol%) showing peaks of cyclohexane carbonate (18% conversion) at room temperature. [# indicates Tetrabutyl ammonium bromide (TBAB) peaks].

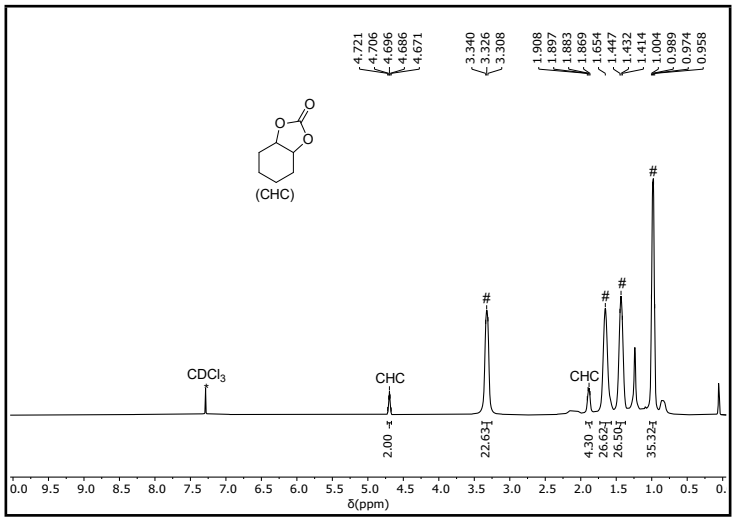

Fig. S57: ^{1}H NMR Spectrum in $CDCl_3$ obtained for a reaction mixture taken after 22 hrs (**Co-1^{H}**: 1.5 mol%, TBAB: 5 mol%) showing peaks of cyclohexane carbonate (>99 % conversion) at 70^0c. [# indicates Tetrabutyl ammonium bromide (TBAB) peaks].

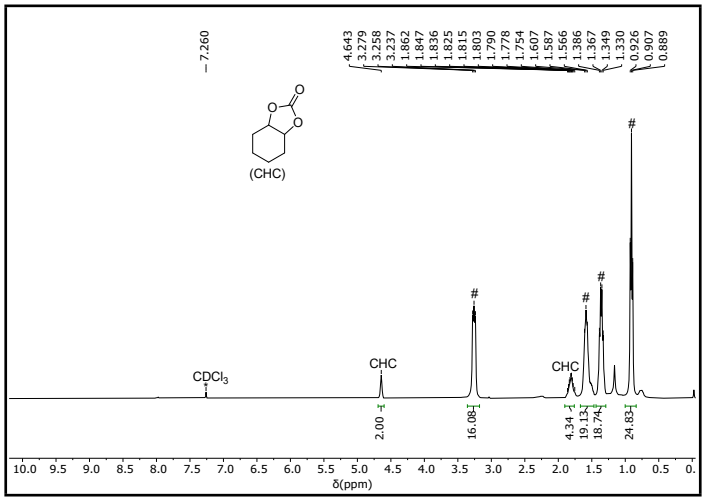

Fig. S58: ^{1}H NMR Spectrum in $CDCl_3$ obtained for a reaction mixture taken after 22 hrs (**Co-1^{Br}**: 1.5 mol%, TBAB: 5 mol%) showing peaks of cyclohexane carbonate (>99 % conversion) at 70^0c. [# indicates Tetrabutyl ammonium bromide (TBAB) peaks].

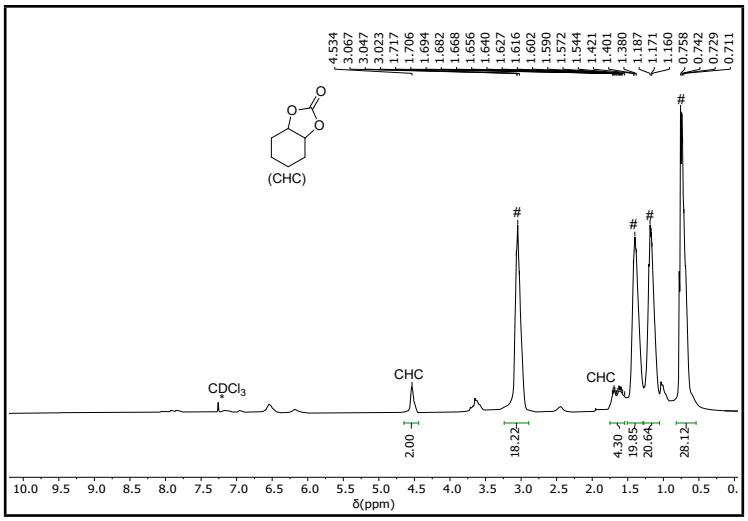

Fig. S59: ^{1}H NMR Spectrum in $CDCl_3$ obtained for a reaction mixture taken after 22 hrs (**Co-1^{NO2}**: 1.5 mol%, TBAB: 5 mol%) showing peaks of cyclohexane carbonate (>99 % conversion) at 70^{0}c. [# indicates Tetrabutyl ammonium bromide (TBAB) peaks].

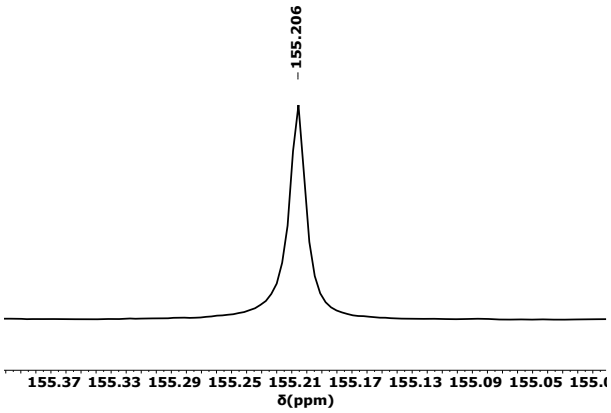

Fig. S60: Carbonyl region of ^{13}C NMR spectrum of cyclohexane carbonate synthesized using **Co-1^{H}**.

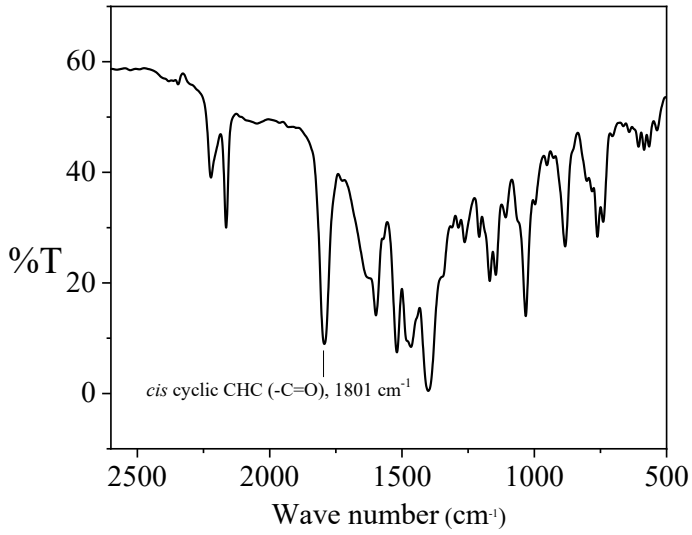

Fig. S61: FT-IR spectrum of cyclic cyclohexane carbonate (*cis*) synthesized using **Co-1^{H}** .

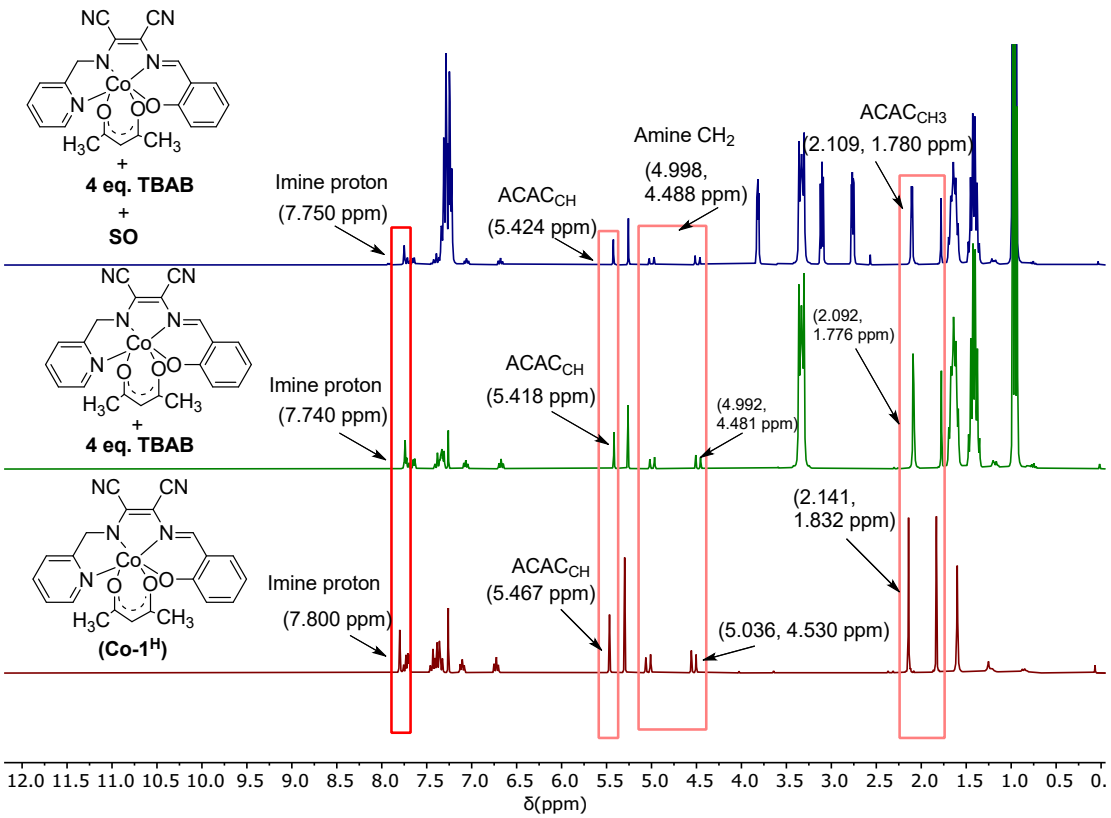

Fig. S62: Comparison between the ^{1}H NMR spectra of complex Co-1^H (bottom), Co-1^H in the presence of 4 equiv. TBAB (Middle) and Co-1^H in the presence of 4 equiv. TBAB and 10 eq. SO (Top) in $CDCl_3$ (δ_H 7.26 ppm).

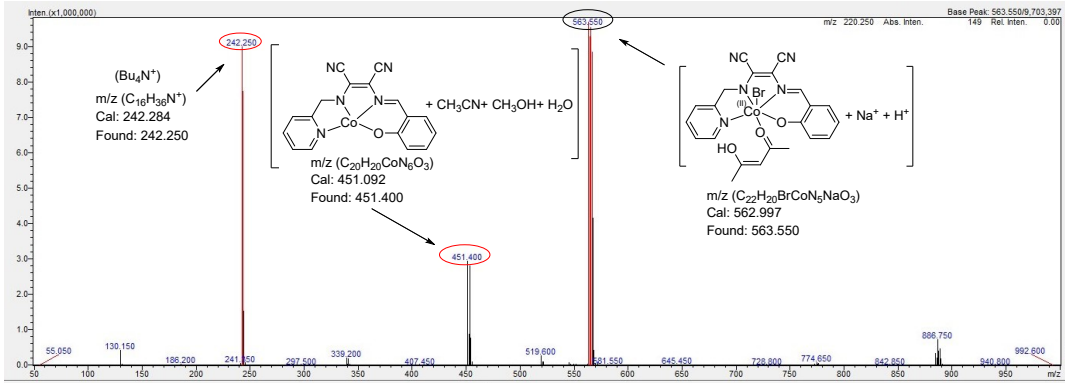

Fig. S63: ESI-MS spectrum of the reaction mixture of [Co(L^H)(acac)] with excess TBAB.

Table S1: Crystallographic data parameters.

Compound ID	**Co-1^{H}**	**Co-1^{Br}**	**Co-1^{NO2}**
CCDC number	2314645	2314644	2314643
Empirical formula	$C_{22}H_{18}CoN_5O_3$	$C_{22}H_{17}BrCoN_5O_3$	$C_{23}H_{19}Cl_2CoN_6O_5$
Formula weight	459.34	538.24	589.27
Temperature/K	100.0(2)	100.0(2)	100.0(2)
Crystal system	triclinic	triclinic	triclinic
Space group	P-1	P-1	P-1
a/Å	8.8732(16)	11.372(3)	10.2770(5)
b/Å	10.2837(19)	11.481(4)	11.8990(6)
c/Å	14.993(3)	12.108(4)	12.2515(6)
α/°	78.404(4)	76.880(5)	63.338(2)
β/°	79.175(4)	62.834(4)	81.714(2)
γ/°	66.066(4)	80.875(5)	70.818(2)
Volume/Å^3	1216.3(4)	1367.1(7)	1264.54(11)
Z	2	2	2
ρ_{calc}g/cm^3	1.254	1.308	1.548
μ/mm^{-1}	0.735	2.117	7.674
F(000)	472.0	540.0	600.0
Crystal size/mm^3	0.09 × 0.08 × 0.08	0.2 × 0.15 × 0.12	0.12 × 0.1 × 0.09
Radiation	MoKα (λ = 0.71073)	MoKα (λ = 0.71073)	CuKα (λ = 1.54178)
2Θ range for data collection/°	5.274 to 54.504	3.65 to 50.674	9.11 to 133.4
Index ranges	-11 ≤ h ≤ 11, -13 ≤ k ≤ 13, -19 ≤ l ≤ 19	-13 ≤ h ≤ 13, -13 ≤ k ≤ 13, -14 ≤ l ≤ 14	-12 ≤ h ≤ 12, -14 ≤ k ≤ 14, -14 ≤ l ≤ 14
Reflections collected	29507	28210	21742
Independent reflections	5220 [R_{int} = 0.0483, R_{sigma} = 0.0314]	4970 [R_{int} = 0.0663, R_{sigma} = 0.0502]	4392 [R_{int} = 0.0645, R_{sigma} = 0.0470]
Data/restraints/parameters	5220/0/282	4970/0/291	4392/0/309
Goodness-of-fit on F^2	1.073	1.042	1.064
Final R indexes [I>=2σ (I)]	R_1 = 0.0411, wR_2 = 0.1153	R_1 = 0.0366, wR_2 = 0.0832	R_1 = 0.0456, wR_2 = 0.1169
Final R indexes [all data]	R_1 = 0.0472, wR_2 = 0.1217	R_1 = 0.0603, wR_2 = 0.0917	R_1 = 0.0483, wR_2 = 0.1184
Largest diff. peak/hole / e Å^{-3}	0.26/-0.81	0.46/-0.47	0.45/-0.52